applied sciences

MDPI

Review

Review of 3D Printing of Polyaryletherketone/Apatite Composites for Lattice Structures for Orthopedic Implants

Reshma McMullan [1,*], Atefeh Golbang [1], Kristine Salma-Ancane [2,3], Joanna Ward [1], Krzysztof Rodzen [1] and Adrian R Boyd [1,*]

[1] School of Engineering, Ulster University, York Street, Belfast BT15 1ED, UK; a.golbang@ulster.ac.uk (A.G.); je.ward@ulster.ac.uk (J.W.); kp.rodzen@ulster.ac.uk (K.R.)
[2] Institute of Biomaterials and Bioengineering, Faculty of Natural Sciences and Technology, Riga Technical University, Paula Valdena, St 3, k-1, LV-1048 Riga, Latvia; kristine.salma-ancane@rtu.lv
[3] Baltic Biomaterials Centre of Excellence (BBCE), Headquarters at Riga Technical University, LV-1048 Riga, Latvia
* Correspondence: monachan-r@ulster.ac.uk (R.M.); ar.boyd@ulster.ac.uk (A.R.B.)

Abstract: Neck and lower back pain, often caused by spinal disorders such as scoliosis and degenerative disc disease, affects over 80% of the global population, with an estimated from 250,000 to 500,000 spinal cord injuries occurring annually according to the WHO. As the demand for spinal procedures continues to rise, advancements in implant materials have become essential. Orthopedic implants play a vital role in restoring mobility and improving the quality of life of patients with musculoskeletal disorders. Metallic implants, such as stainless steel, titanium, and its alloys, are commonly used to make fixation devices for spinal fusion surgery due to their excellent mechanical properties. However, complications such as stress shielding have been recorded. Polymeric materials offer new prospects as an alternative to metal-based materials such as those based on Polyaryletherketone (PEAK). Among the advanced materials used in these implants, PAEK has emerged as the preferred choice due to its exceptional mechanical strength, thermal stability, and chemical resistance. Polyetheretherketone (PEEK) and Polyetherketoneketone (PEKK) offer notable advantages, such as radiolucency and mechanical properties resembling those of natural bone, reducing stress shielding and facilitating postoperative imaging. Although PEEK and PEKK are considered as bioinert, it has been demonstrated that adding bioactive agents such as hydroxyapatite (HA) into the matrix to make composites solves this problem and can help with aiding direct bone apposition. Furthermore, PAEK's compatibility with 3DP enables the creation of patient-specific implants with intricate geometries, enhancing the surgical outcomes. In addition, the lattice structures of orthopedic implants can alleviate stress shielding, provide an enhanced surface area for the release of bioactive agents (or antimicrobial materials), and eliminate more imaging artifacts compared to that of simple, solid metal implants. PAEK/HA composite implants represent a transformative solution, addressing the psychological, social, and economic burdens of spinal disorders, while enhancing the surgical outcomes. With continuous technological evolution, PAEK/HA composites are poised to play a pivotal role in modern spinal care.

Keywords: polyaryletherketone; PEEK; PEKK; 3D printing; spinal implants; lattice structures; advanced manufacturing; bone

Academic Editor: Maria Amélia Ramos Loja

Received: 20 December 2024
Revised: 28 January 2025
Accepted: 6 February 2025
Published: 10 February 2025

Citation: McMullan, R.; Golbang, A.; Salma-Ancane, K.; Ward, J.; Rodzen, K.; Boyd, A.R. Review of 3D Printing of Polyaryletherketone/Apatite Composites for Lattice Structures for Orthopedic Implants. *Appl. Sci.* **2025**, *15*, 1804. https://doi.org/10.3390/app15041804

1. Introduction

Orthopedic implants are the cornerstone of modern medicine, offering critical solutions to restore mobility and improve the quality of life of patients with musculoskeletal disorders.

Among the materials used in these implants, Polyaryletherketone (PAEK) has emerged as the leading choice due to its remarkable combination of properties. PAEK stands out for its exceptional mechanical strength, high thermal stability, and resistance to chemical degradation, making it particularly suitable for long-term orthopedic applications [1]. Polyetheretherketone (PEEK) and Polyetherketoneketone (PEKK) belong to the PAEK family. The key advantage of PAEK is its compatibility with advanced manufacturing techniques such as 3D printing. This capability allows for the creation of highly precise, patient-specific implants with complex geometries, which are difficult to acquire using the traditional manufacturing methods [2]. PAEK implants are especially valuable in orthopedic surgery, where tailored designs can enhance the patient outcomes by ensuring a better fit and function. Unlike metallic implants, PAEK's radiolucency makes it easier for surgeons to monitor healing progress postoperatively using imaging techniques. The traditional metallic implants have been widely used in orthopedic surgery, but they come with notable limitations, including stress shielding, poor bioactivity, and compromised postoperative imaging quality. Stress shielding occurs when metallic implants, which are much stiffer than natural bone tissues, bear too much load, potentially leading to bone resorption and the weakening of the surrounding tissue. Additionally, the non-radiolucent nature of metals often interferes with the imaging techniques, making it difficult to monitor healing post-surgery. PEEK and PEKK offer a promising alternative to these metallic implants by addressing many of the shortcomings of metallic implants.

Unlike metals, PEEK and PEKK are radiolucent, allowing for clear imaging, and their mechanical properties more closely resemble those of natural bone, reducing the risk of stress shielding. However, with these advantages, they present their own set of challenges. Among them is their hydrophobic nature, which limits cell adhesion and impairs osseointegration, making it difficult for the implant to effectively bond with the surrounding bone tissue. To overcome this issue, other researchers have explored the incorporation of bioactive agents such as hydroxyapatite (HA) into PEEK and PEKK. HA is a calcium phosphate-based biomaterial that is widely recognized for promoting bone growth and osseointegration, and it has been successfully used in coatings for hip and knee replacement implants [3]. When HA particles are evenly distributed within the PEEK matrix, the implants can benefit from the bioactivity of HA, while maintaining the structural advantages of PEEK. This composite design allows for HA to be exposed on the implant surface, facilitating better integration with the bone and promoting faster healing [4]. In addition to the use of HA, implant design, such as the creation of porous scaffolds, is showing promise in improving PEEK's performance in orthopedic applications [5]. Porous scaffolds encourage tissue regeneration by allowing soft tissues to grow into the implant, further enhancing the integration of PAEK implants within the body. Together, these innovations are helping circumvent the limitations of the traditional PAEK implants, pushing the boundaries of what is possible in orthopedic surgery and improving patient outcomes [6].

Neck and lower back pain has significant psychological, economic, and social burdens, which can be caused by several factors, such as accidents, injuries, or spinal disorders like scoliosis, congenital deformities, and degenerative diseases, affecting over 80% of the population [7–9]. These conditions strain healthcare systems like the National Health Service, which spends GBP 26 million annually on spinal fusion surgeries aimed at improving patients' quality of life [7]. According to a World Health Organisation (WHO) report, there are from 250,000 to 500,000 spinal cord injuries every year around the world [10]. Factors like spine degeneration, fractures, and conditions such as a herniated disc contribute to nerve compression [10]. Spinal fusion surgery, first performed in 1911 by Dr. Russell Hibbs, is now a common orthopedic procedure worldwide [11]. The rise in spinal fusion surgeries

has driven the spinal implant market due to the aging population and advances in technology. For instance, between 2005 and 2015 in the UK, we saw a 63% increase in spinal fusion surgeries, while those in the US experienced a 77% rise from 2002 to 2011 [12]. In Australia, the incidence of spinal fusions increased by 169% between 1997 and 2006 [11]. The global spinal implants market, valued at USD 13.3 billion in 2023, is projected to grow at a CAGR of 5.4% until 2032, with similar growth rates forecasted by market intelligence platforms.

As the demand for spinal procedures, particularly spinal fusion surgeries, continues to rise, advancements in implant materials have become essential to improve patient outcomes. PAEK implants represent a significant advancement in spinal surgeries, improving the quality of life of patients and reducing the psychological, social, and economic burdens of spinal disorders. As technology continues to evolve, the adoption of PAEK materials will further enhance the surgical outcomes, solidifying their importance in modern spinal care.

2. Natural Bone, Spinal Anatomy and Spinal Fusion

The two types of tissue that comprise bones are compact (cortical) and cancellous (trabecular or spongy) bones. Compact bone, which forms the outer layer of bone, is a dense and durable tissue that makes up around 80% of adult bone mass. It forms the dense outer shell of the vertebrae and has a porosity of between 5 and 15%. Cancellous bone, on the other hand, makes up the remaining 20% of bone and is characterized by its lighter and less-dense nature, as well as its network of rod-like structures known as trabeculae [13].

When designing scaffolds, it is critical to consider the hierarchical structure of bones, their ability to bear mechanical stress, and factors like cell proliferation, adhesion, and osteogenic differentiation. Table 1 below shows the mechanical properties of human bones.

Table 1. Mechanical properties of compact and trabecular bones.

Material	Elastic Modulus (GPa)	Compressive Strength (MPa)	Tensile Strength (MPa)
Compact bone [14]	17–30 (L) 6–13 (T)	130–224 (L) 106–131 (T)	78–151 (L) 50–66 (T)
Trabecular Bone [14,15]	0.05–0.5	4–12	-

(L): longitudinal; (T): transverse.

The spine serves as the central support structure for the human body, linking various components of the musculoskeletal system. The spine enables fundamental movements, such as sitting, standing, walking, twisting, and bending. However, conditions such as spinal cord disorders, back injuries, and other issues can harm the spine and result in back pain [16,17].

Spinal fusion surgery is a major surgical process, and the decision to undergo it is typically considered only after conservative treatment, including medications and therapy, have been explored, considering the patient's overall health. A typical spinal fusion procedure involves the joining of two or more vertebrae together so that there is no movement between them, and over time they heal to form a solid unit. The process involves the bones between two adjacent vertebrae being roughened, and then a graft is placed between them [18]. Plastic or metal spacers may be used to replace the disc materials. Until fusion or the bone regrows, rods and screws are placed to create an internal cast that holds and supports the vertebrae [18]. The primary concern associated with any spinal fusion surgery is the inability to alleviate back pain, a scenario observed in at least 20% of spinal fusion surgeries conducted in both the UK and the USA [18,19]. Another postoperative risk involves the potential failure of the vertebrae to successfully fuse via the bone graft, potentially leading to pseudoarthrosis. From approximately 5 to 10% of spinal fusion

surgery patients experience suboptimal outcomes despite the application of contemporary techniques [18,19].

The biomaterials used in spinal surgeries must meet several criteria, including sufficient strength, excellent corrosion resistance, bioadhesion, biofunctionality, biocompatibility, high wear resistance, and low friction. Some of the biomaterials which have been developed do not satisfy all the requirements mentioned above due to the nature of the materials. Corrosion and wear are two major issues that have been reported as the primary reasons for failure. Metallic implants, such as titanium (Ti), stainless steel, and cobalt (Co)–chromium (Cr) (Co-Cr) alloys, are commonly used to make fixation devices for spinal fusion surgery due to their excellent mechanical properties. The properties of biomaterials compared with those of natural bone are detailed in Table 2.

Table 2. Mechanical properties of biomaterials [20].

Material	Young's Modulus (GPa)	Yield Strength (MPa)	Tensile Strength (MPa)	Fatigue Limit (MPa)
Stainless steel	190	221–1213	586–1352	241–820
Co-Cr alloys	210–253	448–1606	655–1896	207–950
Titanium (Ti)	110	485	760	300
Cortical Bone	15–30	30–70	70–150	-

Complications such as stress shielding were observed due to materials such as titanium being stiffer than natural bone. Metal debris circulates in the body and accumulates in the organs, which can be fatal [21]. In revision procedures for individuals who have undergone posterior lumbar instrumentation, and subsequently developed pseudoarthrosis, metal debris has been discovered in soft tissues surrounding the paraspinal area [22]. The failure of implants can arise from various factors, including wear and corrosion, fibrous encapsulation, inflammation, low fracture toughness, and a mismatch in the modulus of elasticity between the implant and the surrounding bone. These issues can compromise the structural integrity and biomechanical compatibility of the implant, leading to long-term complications. Over time, these problems may result in mechanical failure, such as the cracking or fracturing of the implant. Such failures often necessitate revision surgery, which poses additional challenges for patients, including prolonged recovery times, increased medical costs, and a higher risk of complications. Ensuring that implants are designed with optimal materials and mechanical properties is critical to minimize these risks and improve their long-term success rates [23].

Elements such as Nickel (Ni), chromium (Cr), and cobalt (Co) in both Co-Cr alloys and stainless steel have been found to have toxic effects. Ni toxicity in the body can cause dermatitis, and carcinogenic effects are caused by using Co [24]. Additionally, a high friction coefficient and wear debris formation can produce an inflammatory reaction, leading to the loosening of implants due to osteolysis. Metallic implants can cause signal artifacts in Magnetic Resonance Imaging (MRI), Computed Tomography (CT), and X-ray images. In CT and X-ray images, this primarily occurs because X-rays are attenuated by the metal along the beam path [24]. In MRI imaging, artifacts are introduced due to interference with the magnetic field, which can cause distortions and affect the quality of the scan [25].

3. Polyaryletherketone

A new alternative to metal-based materials is polymeric biomaterials such as those based on PAEK [26]. PAEK is a semicrystalline, thermoplastic polymer that contains both ether and ketone groups. Its structure gives it a glass transition temperature of around 157 °C and a melting point of 370 °C. The physical properties of PAEK are affected by the ratio and arrangement of ether and ketone groups, with a greater number of ketone groups

leading to increased polarity and stiffness. As a result, both the glass transition temperature and the melting point are higher [1].

Polyetheretherketone (PEEK) and Polyetherketoneketone (PEKK) are two materials that belong to the PAEK family. Both the materials have high-temperature resistance, fatigue resistance, and have the ability to be sterilized, making them perfect candidates for healthcare applications [27–29]. In contrast to metals, PAEKs do not cause artifacts in CT/MRI scans. However, their material composition can lead to differences in certain characteristics, such as their degree of crystallinity and the speed of crystallization [30]. Figure 1 shows the structures of PEEK and PEKK.

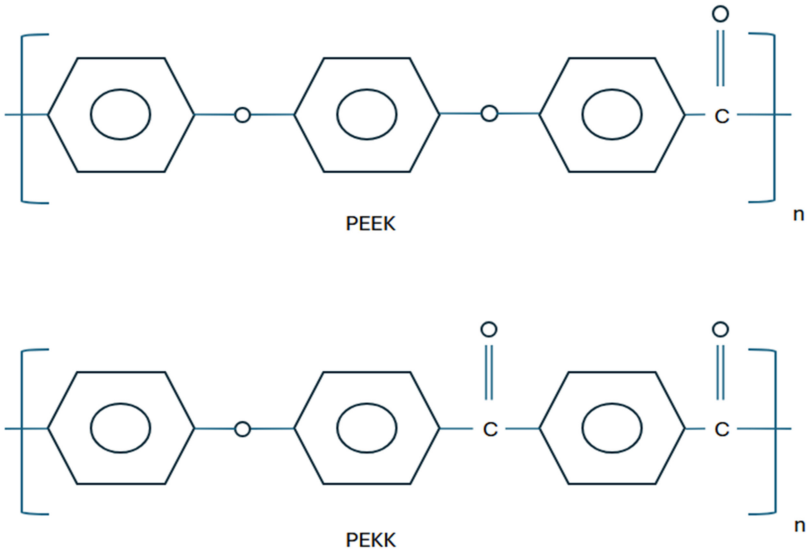

Figure 1. Structures of PEEK and PEKK [1].

As described by Labdhi et al. and Syazwani et al., PEEK is a semicrystalline, thermoplastic, polycyclic, aromatic polymer synthesized through the reaction of 4,4′-difluorobenzophenone with disodium hydroquinone at 300 °C, with a melting point of 335 °C [1]. PEKK, on the other hand, is synthesized from diphenyl ether and terephthaloyl chloride, with aluminum chloride and nitrobenzene used as catalysts. The key difference between PEKK and PEEK lies in the presence of an additional ketone group in PEKK's aromatic ring. This structural variation increases the polarity and backbone rigidity of the material [1,31].

PEEK and PEKK share physical and mechanical characteristics that resemble those of bone, resulting in high impact resistance [1]. Tables 3 and 4 compare the properties and differences of PEEK and PEKK.

Table 3. Properties of PEEK and PEKK [1].

Properties	PEEK	PEKK
Physical Properties	Biocompatible, minimal plaque affinity, aesthetics, dimensional stability, good polishability, and wear resistance	Biocompatible, shock absorbance, aesthetics, flexibility, microporosity, and hydrophilic nature
Tensile Strength (MPa)	101	115
Elastic Modulus (GPa)	3.5	5.1
Flexural Strength (MPa)	164	200
Compressive Strength (MPa)	118–169	246
Melting Temperature (°C)	334–350	363–386
Water Absorption (mg/mm^3)	0.1–0.5	8.7

Table 4. Differences between PEEK and PEKK [1].

PEEK	PEKK
Contains two ether groups and one keto group	Contains two keto groups and one ether group
Higher extrusion temperature (almost 400 °C)	Lower extrusion temperature (340 °C–360 °C)
Lower glass transition temperature (143 °C)	Higher glass transition temperature than PEEK (159 °C)
Low modulus of elasticity than PEKK	Greater modulus of elasticity than PEEK
80% straight and 20% kinked segments melt at 360 °C	60% straight and 40% kinked segments melt at 305 °C

3.1. Polyetheretherketone (PEEK)

PEEK has gained attention for its potential use in orthopedic implants due to its exceptional biocompatibility, chemical resistance, sterilizability, and mechanical properties, such as stiffness and strength, which closely mimic those of human bone [28,30]. Additionally, PEEK does not present the same issues, with local inflammation and stress shielding commonly associated with metallic implants, making it a promising biomaterial [28]. PEEK has already been applied in various fields, including spinal fusion cages, dental implants, and maxillofacial reconstruction [27]. PEEK demonstrates exceptional mechanical strength, largely attributed to its polymer structure, which provides rigidity and resilience under stress [32]. This makes PEEK particularly well suited for applications in spinal implants, where it must endure significant mechanical loads over time without deforming or breaking down. Its durability allows for PEEK implants to effectively support the spine, even in cases of high-level stress or strain, such as those experienced during movement or physical activity [32,33]. In addition to its mechanical robustness, PEEK's radiolucent nature sets it apart from the traditional metallic implants. This property allows for clearer radiographic imaging, which is crucial for evaluating bone fusion after spinal surgery. Unlike metallic implants that can obscure the imaging results, PEEK enables surgeons to closely monitor the healing process and assess the effectiveness of spinal fusion procedures without interference. It is particularly valuable in postoperative care, as it allows for more accurate diagnostics and timely interventions if needed [26,29,32,33]. The combination of high mechanical strength and radiolucency makes PEEK an ideal material for spinal implants, where both the load-bearing capacity and the ability to monitor bone healing are critical to patient outcomes [34,35]. Ongoing advancements in PEEK-based technologies, such as surface modifications and bioactive coatings, continue to enhance their performance, making them an increasingly popular choice in spinal and orthopedic surgeries [4,36,37].

PEEK is considered bioinert due to its poor integration with surrounding tissues [27,28]. However, various methods have been proposed to make PEEK bioactive [28,38,39]. Several methods have been proposed to improve the bioactivity of PEEK, such as chemical or plasma treatment to modify the surface, coating with plasma spraying or sputtering, and the direct fabrication of composite materials with bioactive agents through injection molding or 3D printing [27,39,40]. One such method involves the manufacturing of composite materials and the addition of bioactive agents such as hydroxyapatite (HA) into PEEK. It has been demonstrated that this approach could provide a suitable solution [27,41,42]. HA belongs to the apatite family, a group of crystalline compounds with a hexagonal lattice structure [43]. The primary applications of synthetic HA $Ca_{10}(PO_4)_6(OH)_2$ are bone graft material to fill bone defects, bioactive implant coatings, dental surgery materials, and craniofacial and maxillofacial reconstruction materials particularly [44]. It is considered that synthetic HA has similarities to bone apatite in terms of chemical composition, structure, and size, and these features can provide exceptional osteoconductive and osteointegrative characteristics [41,45–47]. Compared to those of other bioactive ceramic glasses (such as Bioglass®) or A-W glass-ceramics, the primary advantage of employing HA as a biomaterial or bioceramic is its chemical resemblance to the inorganic constituents of bone and teeth [41]. It is primarily utilized in the repair of hard tissues such as bones and can be employed

in bone augmentation procedures; as coatings for implants, like total hip replacement (THR) or total knee replacement (TKR); as fillers for bones or teeth; as matrices for drug release control; and in the production of scaffolds suitable for tissue engineering (TE) applications [48]. The presence of porous HA coatings on metallic implants facilitates and enhances tissue ingrowth, resulting in the improved mechanical stability of the implant in the surrounding bone [49]. Others have stated that orthopedic implants made from additively manufactured PEEK possess several advantages, such as biocompatibility and similar density and mechanical properties to those of natural bone [50]. The successful use of PEEK implants relies on the integration of both bone tissue and soft tissue with the implants [51]. Some studies have investigated a variety of bioactive agents as additives for composites based on PEEK: HA [36,37,52–55], strontium (Sr)-substituted apatites [56], fluoro-hydroxyapatite [52,57], β-tricalcium phosphate [β-TCP $Ca_3(PO_4)_2$] [52], calcium silicate [36,53], Bioglass® [54], and titanium dioxide (TiO2) [55]. While adding bioactive agents to the PEEK matrix to create composite materials has clear advantages, it is important to note that these additives have the potential to alter bone homeostasis and could be toxic to osteoblasts, depending on their concentration and size (micro- versus nanoparticles). Therefore, the potential risks associated with using these biomaterials should be carefully considered when selecting a composite material [36,52–56]. While HA is biocompatible and osteoconductive, it exhibits poor rates of resorption and low mechanical strength. Its stoichiometry is variable, and it can undergo various cationic substitutions to enhance its biological and physical properties [49].

3.2. Polyetherketoneketone (PEKK)

Polyetherketoneketone (PEKK) is an advanced, high-performance polymer that has garnered widespread attention for its exceptional properties and versatility, particularly within the biomedical field [58]. Initially introduced by Bonner in 1962 [59], PEKK was first employed in the industrial and military fields due to its robust mechanical and thermal characteristics [58]. In recent years, however, significant advancements in material science and manufacturing technologies have shifted the focus toward its potential as a biomaterial, driving innovation in medical and dental applications [58,60]. What sets PEKK apart is its outstanding mechanical strength, excellent chemical resistance, and high thermal stability, all of which position it as a leading material among thermoplastic composites. This methacrylate-free thermoplastic offers remarkable shock absorption and fracture resistance, making it a reliable choice for demanding environments. With an elastic modulus of 5.1 GPa, PEKK outperforms its counterpart, PEEK, offering enhanced strength and elasticity that are critical in load-bearing applications [61]. A notable feature of PEKK is its similarity to human bone in terms of density and elastic modulus, which significantly reduces the risk of bone resorption when used in implants [62]. This unique compatibility makes it particularly well suited for orthopedic and cranial applications [63]. Furthermore, the presence of an additional ketone group in its molecular structure provides an avenue for enhanced surface chemical modifications, enabling tailored interactions with biological environments and expanding its scope of application [58].

In the fields of orthopedics and dentistry, PEKK has emerged as a transformative material, demonstrating its value in restorative, prosthetic, and implant procedures. Its biocompatibility, combined with exceptional mechanical properties, has established it as an ideal material for cranial reconstruction and mandibular implants [59,60,64]. The integration of AM technologies such as 3D printing has further amplified its potential [65]. These methods facilitate the creation of intricate, patient-specific implants, such as custom bone analogues designed for mandibular reconstruction, offering a level of precision and adaptability previously unattainable [64]. PEKK's adoption in spinal fusion procedures

underscores its growing role as a reliable, implantable-grade material [59]. Its superior thermal stability, mechanical resilience, and ease of surface modification have made it the preferred choice for high-demand biomedical applications [58,65]. As the demand for advanced biomaterials continues to rise, PEKK is poised to play a pivotal role in the developing next-generation medical devices and implants [58]. Table 5 shows the mechanical properties of PEEK, PEKK, and Ti.

Table 5. Mechanical properties comparing PEEK, PEKK, and titanium [30,60,66].

Properties	PEKK	PEEK	Ti	Reference
Tensile strength (MPa)	115	100.69	240–890	[30,60,66]
Elastic modulus (GPa)	5.1	3.5	103–114	[30,60,66,67]
Compressive strength (MPa)	246	118–169	130–170	[30,60,66]
Melting temperature (°C)	363–386	334–350	1650–1670	[30,60,66]
Flexural strength (MPa)	200	164	65	[30,60,66]
Density (g/cm^3)	FEFF1.3	1.3	4.4–4.5	[30,60,66]

4. Additive Manufacturing—3D Printing and 3D Printers

Additive manufacturing (AM), commonly known as 3D printing (3DP), is a process that creates a customized, three-dimensional (3D) object layer-by-layer from digital data created using Computer-Aided Design (CAD) Software [68]. This transformative technology has received significant attention across diverse industries due to its flexibility, speed, and ability to produce complex geometries that were previously challenging or impossible with the traditional manufacturing methods [50]. AM offers numerous advantages compared to the traditional subtractive manufacturing. The layer-by-layer process not only yields environmental and lean manufacturing benefits by minimizing material waste, but also allows for design freedom, enabling the production of complicated geometries and customization that would be considered 'unmanufacturable' using the conventional methods. Additionally, AM boasts rapid prototyping capabilities and material versatility and reduces the use of costly equipment such as molds [2]. Over the last decade, significant advancements in material diversity, design flexibility, printing techniques, speed, and cost within the realm of 3DP have played a catalyzing role in propelling Industry 4.0 and personalized medicine forward [69]. This transformative progress has revolutionized the healthcare sector by transitioning pharmaceutical manufacturing from mass production to an on-demand, personalized model [70].

AM encompasses various types of 3D-printing technology, each employing unique techniques to create 3D objects. Stereolithography (SLA), developed by Charles Hull in 1986, was one of the first methods and marked the beginning of modern 3D printing. SLA utilizes ultraviolet (UV) light to cure liquid photopolymer resin layer-by-layer into solid objects [71]. Since then, numerous advancements have been made, resulting in technologies tailored for diverse applications [72]. Inkjet printing uses print heads to deposit binder or material droplets onto a powder bed or directly into the layers, enabling high-speed production and multi-material capabilities. Selective Laser Sintering (SLS) employs a laser to fuse powdered materials like polymers or metals layer-by-layer, producing durable and intricate components widely used in aerospace and automotive industries. Fused Deposition Modelling (FDM), also known as Fused Filament Fabrication (FFF), is one of the most cost-effective methods, involving the extrusion of thermoplastic filament through a heated nozzle to build objects layer-by-layer [73,74]. Digital Light Processing (DLP), similar to SLA, uses a digital light projector to cure entire layers of resin at once, offering faster print speeds. Binder Jetting, involves selectively depositing a liquid binding agent onto a thin layer of powdered material, such as metal or ceramic, to produce components with complex geometries that are later sintered or post-processed. Figure 2 provides a schematic

representation of these diverse 3D-printing technologies, each contributing to the ongoing evolution of additive manufacturing and its expanding range of applications [75].

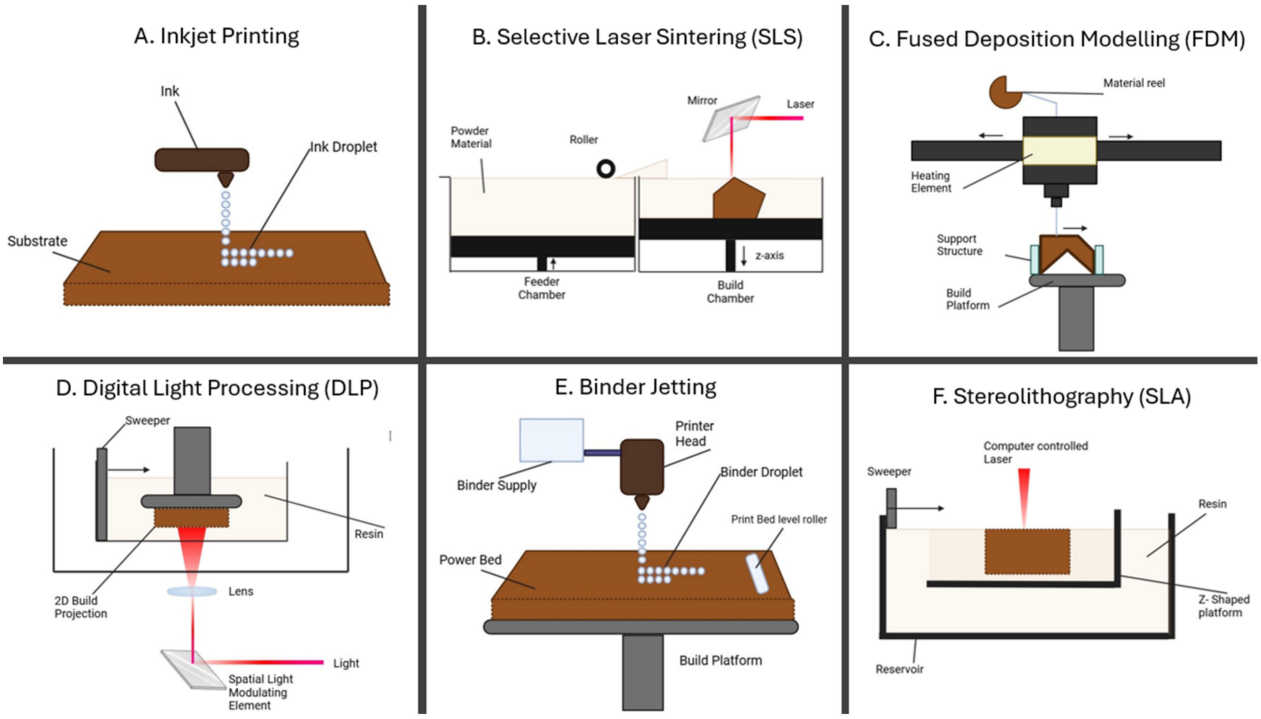

Figure 2. Schematic diagram of different 3D printers.

FFF is one of the most cost-effective methods of 3D printing worldwide. This process involves the use of materials which are heated and extruded layer-by-layer to create a 3D object [76,77]. PAEK and HA powders are carefully blended to ensure the uniform distribution of particles, resulting in a composite material with enhanced mechanical and thermal properties. This mixture is then processed into a continuous filament, which serves as the raw material for the 3D printing process. During printing, the filament is fed into the extruder of the 3D printer, where it is heated to its melting point. The molten composite material is then pushed through a precision nozzle and deposited onto the build platform layer-by-layer, following the predetermined path defined by the CAD model. As each layer is deposited, the material cools and solidifies, gradually forming the desired 3D structure [78]. This method is particularly advantageous for fabricating PAEK composites due to its ability to produce complex geometries with high precision and minimal material wastage [77]. Figure 3 below provides a schematic representation of the FFF process for PAEK composites, illustrating the key steps involved in transforming the composite filament into the final printed object.

Several factors and parameters must be carefully considered when 3D printing to ensure a successful outcome. Each parameter, such as the print speed and the nozzle temperature, plays a critical role in determining the final quality of the print, the printing time, and the overall cost [79]. These parameters need to be configured accurately to achieve a high-quality, functional 3D-printed object. The key considerations include layer height, which affects resolution and surface smoothness, with smaller heights offering finer details but increasing printing time. The print speed influences both quality and production time, as slower speeds improve precision, while higher speeds can compromise detail [80]. The nozzle temperature must be set appropriately for the material being used to ensure smooth extrusion and prevent clogging or under-extrusion [81]. The bed temperature is equally important for maintaining proper adhesion of the first layer, especially for materials like

PAEK, which are prone to warping [82]. Support structures are necessary for overhangs or complex geometries to prevent failure during printing, while adhesion to the bed can be improved using a heated bed, adhesive materials, or techniques like adding a raft or a brim [83]. Additionally, the flow rate must be finely tuned to avoid over-extrusion, which leads to blobs and rough surfaces, or under-extrusion, which results in weak and incomplete prints [80,84]. By carefully calibrating these factors based on the material, printer model, and design requirements, you can optimize the process and produce a high-quality, 3D-printed object.

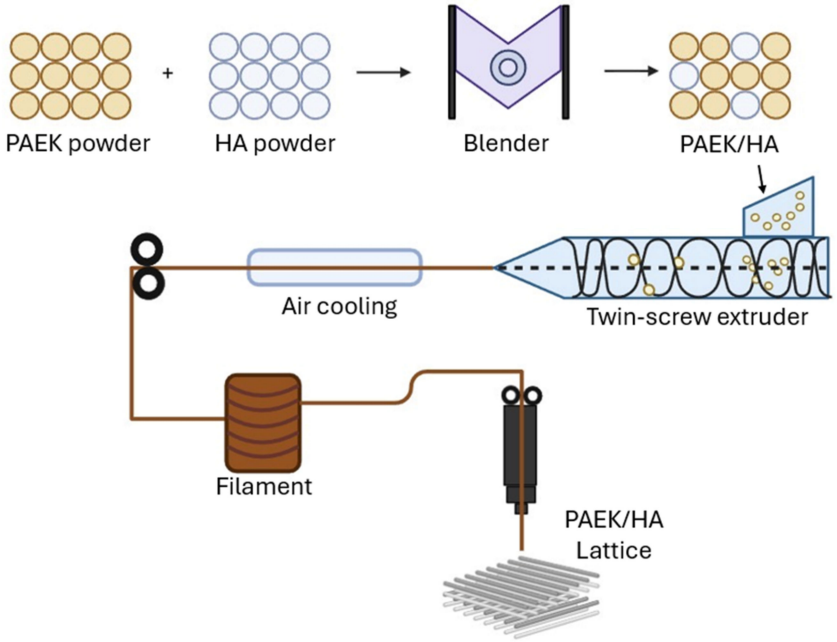

Figure 3. Schematic diagram showing FF process of PAEK composite.

As detailed by in the literature and Table 6, orthopedic implants made through AM using PAEK exhibit notable advantages, including exceptional biocompatibility and properties such as density and mechanics comparable to those of natural bone [50]. The extrusion process utilizes a heated nozzle to melt thermoplastic filaments, which are then precisely deposited according to a programmed design. This technique allows for fabricating intricate and customized objects with relative ease and cost-effectiveness. Wittbrodt et al. have explored the potential of open source 3DP with extrusion-based systems, emphasizing accessibility and affordability [4,85]. Additionally, the work of Bellini and Güçeri sheds light on the material considerations and process parameters involved in extrusion-based AM [73]. Extrusion-based techniques play a pivotal role in the democratization of manufacturing, making it accessible to a wider audience, while contributing to the ever-expanding applications of AM technologies.

Table 6. Table showing advantages and disadvantages of 3D printing of PAEK implants.

Category	Advantages	Disadvantages	References
Mechanical Properties	Lightweight, mimicking the strength of human bone and reducing stress shielding.	May have weaker load-bearing properties compared to traditional metals like titanium.	[4,67]
Biocompatibility	Minimal inflammatory, enhances tissue integration.	Risk of poor integration or delamination over time in some cases.	[50,86]

Table 6. *Cont.*

Category	Advantages	Disadvantages	References
Customization	Patient-specific implants tailored to anatomical structures, improving fit and surgical outcomes.	Producing consistent and high-quality customized implants requires advanced equipment and expertise.	[87]
Imaging	Radiolucent, enabling clear CT, X-ray, and MRI imaging for postoperative evaluations.	Nonspecific, but metals may still be preferred for some high-load imaging cases.	[65,88,89]
Porosity	3D printing allows porous structures, promoting bone ingrowth and spinal fusion.	Achieving optimal porosity and mechanical properties can be challenging and time-consuming.	[65,88–91]
Surface Modifications	Allows customized surface textures or coatings to enhance tissue bonding and bioactivity.	Surface modifications may not always prevent delamination or poor integration.	[63,91]

Advancements in AM are paving the way to produce more complex, patient-specific implant designs, while also improving cost-efficiency. One notable development is the emergence of new 3D printer designs, such as those from the New Dimension 3D printing company, which offer enhanced capabilities for producing intricate, personalized implants [92]. These advancements enable more precise control over the material properties, allowing for the creation of implants tailored to a patient's unique anatomical requirements. In addition to these technological improvements, the cost–benefit analysis conducted by Lee et al. highlights the economic advantages of AM in healthcare settings, particularly for cranial implants [93]. Despite the higher initial cost of 3D printing, another study found that the overall cost was reduced due to factors such as shorter surgical times, fewer postoperative complications, and quicker recovery periods [93]. Specifically, the use of AM reduced the average cost per patient by 15%, considering the savings in operating room time, anesthesia use, and hospital stays [93]. These findings suggest that while the upfront investment in AM technology may be higher, the long-term savings from reduced healthcare resource use make it a cost-effective solution for patient-specific implants.

To accommodate the rapid evolution of 3D-printed implants, while ensuring both safety and innovation, the regulatory standards must evolve to address the unique challenges and opportunities presented by this technology. For high-risk devices, such as orthopedic implants classified as Class III under the EU Medical Device Regulation (MDR), compliance typically requires extensive technical documentation and clinical trials reviewed by a notified body, which can take years [94]. However, customized or patient-specific devices produced via 3D printing often fall under more flexible frameworks, such as annex XIII of the MDR [94]. These frameworks allow for deviations from the standard safety and performance requirements when sufficient justification is provided, enabling the development of bespoke implants for individual patients without compromising the regulations [94].

Globally recognized standards such as ISO 13485 Medical Devices (ISO—International Organization for Standardization, n.d.; ISO—ISO 13485-Medical Devices, n.d.), which outline requirements for quality management systems in the design and manufacture of medical devices, play a critical role in ensuring consistency and safety in 3D-printed implants [95]. For example, ISO 13485 certification ensures that every step of the manufacturing process from material selection and design considerations to risk analysis and labelling adheres to strict quality control protocols [95,96]. Incorporating these standards, particularly in point-of-care manufacturing, is essential to maintain traceability, minimize the contamination risk, and uphold device quality. In the United States, the FDA regulates 3D-printed devices under its Quality System Regulation (QSR), which is aligned with the ISO 13485 principles [95,96]. The FDA has issued specific guidance on submissions for 3D-printed devices, emphasizing material traceability, design optimization, and adherence

to good manufacturing practices [94,96]. To keep pace with innovation, regulators must streamline approval pathways for patient-matched devices and develop specific guidelines for point-of-care manufacturing facilities to implement ISO 13485-compliant systems. Collaborative efforts between regulators, manufacturers, and healthcare providers are crucial to foster innovation, while ensuring safety [96–98]. By integrating global quality standards, leveraging emerging technologies such as AI and addressing the gaps in oversight, regulatory frameworks can support the growth of 3D-printed implants, while maintaining high standards of patient care and safety [97].

5. Lattice Structures in Medical Devices and Applications

5.1. Lattice in Bone Structures

Some of the key reasons for using lattice structures in bone implants comprise mitigating stress shielding, facilitating drug release, reducing and removing radiographic artifacts, and promoting osseointegration for fixation. Stress shielding occurs when a bone is inadequately loaded, typically because the load is diverted by a rigid implant. This condition can result in bone resorption, ultimately leading to the implant loosening [99]. Utilizing lattices can help mitigate stress shielding by diminishing the stiffness of the implant [100]. As mentioned above, metals are still, to this day, used for spinal fusion implants. This can cause artifacts in MRI, CT, and X-ray images. Substituting solid implants with lattice structures decreases the total volume of metal, thereby eliminating the artifacts in both the cases. Osseointegration is established when there is direct contact between the bone and the implant, creating mechanical stability and forming a structural and functional connection [101]. Several factors associated with implant geometry impact osseointegration. These factors encompass the size of the pores within the structure, although there is limited consensus on the optimal size, with various sources citing anything from 100 to 1000 µm [86,102–104]. The connectivity of pores impacts the availability of vascularization, gas exchange, and the conveyance of nutrients and waste [104,105]. Pores arranged in a structured design, as seen in the reticulating lattice shown in Figure 4, contribute to superior osseointegration compared to that of tortuous ones, while compact pores are prone to becoming occluded [106].

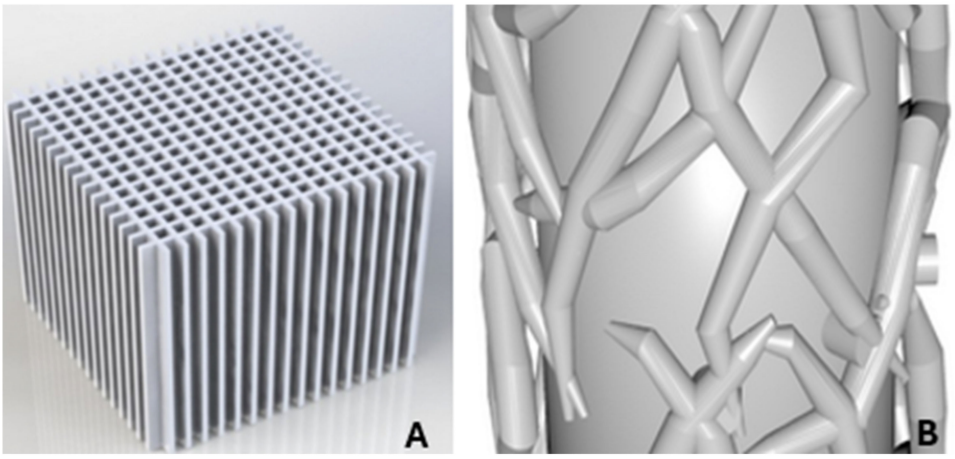

Figure 4. Reticulated lattice image (**A**) vs. stochastic structure image (**B**).

A lattice refers to a cellular framework consisting of solid material intertwined with pores. The cell structure can exhibit either an open or closed configuration, determined by the interconnectedness of the pores with the external environment [6]. According to Dong et al., a lattice structure is characterized as a truss-like configuration with interconnected struts and nodes within three-dimensional space [107,108]. According to Tao et al., a lattice

structure is characterized as an architectural arrangement composed of an array of spatially periodic unit cells, encompassing edges and faces [5].

Open cell lattices are often used in medical applications due to their suitability for fabrication using powder bed fusion techniques. This is attributed to the absence of internal voids, which eliminates the challenge of powder entrapment during the manufacturing process [109]. Additionally, these lattices yield a less rigid structure, which proves advantageous for osseointegration and vascularization, effectively mitigating the impact of stress shielding [110]. The utilization of lattice structures in a lightweight design is common, aiming to reduce material waste and energy consumption during the manufacturing process. Effectively designing and optimizing lattice structures can lead to significant savings in energy, materials, and manufacturing time [108].

A structure with a recurring design can be termed reticulated, whereas structures with a random design are referred to as stochastic, as shown in Figure 4 [111]. Stochastic structures are frequently characterized by heterogeneity, posing challenges in predicting mechanical behavior [112]. These structures may not always align with the design constraints of the printing process. Consequently, reticulating lattices are more commonly employed as implants [113]. Reticulated lattices can be established on a repeating unit known as a unit cell, which can be either surface-based or strut-based [113].

Instances of strut-based lattices encompass those derived from crystal structures like body-centered cubic (BCC) and diamond. Surface lattices, on the other hand, consist of patterns such as gyroid and Neovius sheets [114]. Strut-based lattices can be categorized into structures dominated by bending and stretching, guided by Maxwell's stability criterion. This criterion offers valuable insights into anticipated failure mechanisms [107].

5.2. Stochastic Cellular Structures

Stochastic, open cellular structures apply biomimetic principles to create random pore shapes, sizes, and distributions without a clear, repetitive pattern [115]. These structures aim to mimic the natural variability found in biological tissues, particularly in trabecular bone, which has an irregular and anisotropic architecture [116,117]. The randomness in pore geometry allows for stochastic designs to exhibit anisotropic mechanical responses, meaning their strength and stiffness can vary depending on the direction of the applied load. This characteristic is beneficial for mimicking the load-bearing behavior of trabecular bone, which naturally adapts to directional stresses in the body [115]. Despite these advantages, there are significant challenges associated with the design and manufacturing of stochastic scaffolds, which limit their practical application in orthopedic implants. The complexity of producing these irregular structures, particularly through AM or the traditional fabrication techniques, can lead to inconsistencies in the mechanical properties of the final product. Since the pores and struts of a stochastic structure vary randomly, the scaffold's mechanical performance can be heterogeneous, with areas of varying strength and stiffness [116,118]. This lack of uniformity can compromise the structural integrity of the implant, making it difficult to predict how it will perform under the physiological loads encountered in spinal or other orthopedic applications. Moreover, the inherent heterogeneity of stochastic structures means that certain regions may be more prone to failure than others, particularly under repeated stress or in load-bearing environments. This limitation has hindered the widespread adoption of stochastic designs in orthopedic implants, as their mechanical performance must be reliably consistent to ensure long-term success in clinical applications [115,116].

To address these challenges, other researchers have proposed improving stochastic designs by introducing a hierarchical order into the structure. A hierarchical approach would involve organizing the random pores into multiple levels of scale, like how natural

bone is structured at both the micro and macro levels [119]. This could improve the overall mechanical properties of the scaffold by providing additional layers of support and load distribution, while still retaining the benefits of a biomimetic, anisotropic design. By organizing pores in a controlled, yet random manner along different scales, the scaffold could achieve greater strength and durability, making it more suitable for spinal implants and other orthopedic devices [119]. Hierarchical stochastic designs may also allow for more precise control over critical parameters, such as pore size, distribution, and interconnectivity, which are essential for promoting tissue ingrowth, vascularization, and nutrient flow [119,120]. With these improvements, stochastic cellular structures could overcome their current limitations, providing a more effective solution for mimicking natural bone properties and enhancing the mechanical performance of orthopedic implants.

5.3. Reticulated Cellular Structure

Orthopedic implants often incorporate reticulated structures due to their versatile and adaptable isotropic properties, which are achieved through the repetition of unit cell geometry across the entire scaffold [118–121]. These structures are characterized by their regular and predictable architecture, which repeats a consistent pattern along multiple axes. This uniformity provides a reliable mechanical performance and makes reticulated structures ideal for applications, where consistent load distribution and mechanical strength are critical [118].

Reticulated topologies can be designed with various geometric shapes, ranging from simple forms like cubic, triangular, and honeycomb patterns to more complex shapes, such as dodecahedral and diamond configurations [118,121]. Each geometric shape influences the scaffold's overall compressive strength and mechanical properties. For example, honeycomb and triangular designs are known for their high stiffness and strength, making them suitable for load-bearing applications, while more intricate shapes like dodecahedral and diamond structures may offer enhanced flexibility and better adaptability to different mechanical demands [122,123].

The ability to tailor mechanical properties by adjusting the porosity and orientation of the unit cells is one of the key advantages of reticulated designs. Increasing the porosity of the scaffold can reduce its stiffness, making it more flexible and better aligned with the mechanical behavior of natural bone [124,125]. This reduction in stiffness helps alleviate stress shielding. However, increasing porosity or altering the orientation of unit cells to lower stiffness may also lead to a decrease in the scaffold's ability to withstand compressive forces [124]. This trade-off between flexibility and compressive strength is a critical consideration in the design of reticulated structures for orthopedic implants, particularly in weight-bearing applications like spinal fusion or joint replacement.

The compressive strength of a reticulated scaffold is highly dependent on the geometry of the unit cells and how they are oriented relative to the applied load. For instance, cubic and honeycomb structures may provide higher strength in specific directions, while more complex shapes like dodecahedral structures might offer a more even distribution of forces [118,126]. This flexibility in design allows for engineers to customize the mechanical properties of the implant to meet the specific demands of different anatomical locations [118,124].

5.4. Design Criteria for Cellular Scaffolds in Spinal Implants

For a spinal implant to successfully integrate with surrounding bone tissue and promote vascularization, it must closely mimic the properties of the extracellular matrix (ECM) found in natural tissue. This involves achieving a delicate balance between the implant's functional, morphological, and structural characteristics [88,89]. The ECM provides a

biological framework that supports cell attachment, differentiation, and tissue growth, all of which are crucial for osseointegration. To replicate the ECM, a spinal implant must first meet specific mechanical and structural requirements. It must offer sufficient strength and stability to support the spinal column under physiological loads, ensuring that the implant can bear weight without causing stress shielding [88,89]. At the same time, the implant should possess a porous microstructure that mimics the natural morphology of bone, facilitating the migration of bone cells (osteoblasts) into the scaffold, promoting tissue regeneration. Morphologically, the implant's surface texture and porosity play key roles in encouraging cell adhesion and proliferation. A porous structure not only enhances mechanical interlocking between the bone and the implant, but also allows for the infiltration of blood vessels, essential for delivering nutrients and removing waste products during the healing process [88,89,127]. Vascularization is a critical factor in bone regeneration, as it supports the formation of new bone and ensures the long-term stability of the implant. Moreover, the implant must also achieve a functional balance, wherein it supports both the mechanical load of the spine and the biological processes necessary for healing. This includes ensuring that the material used for the implant is biocompatible, promotes bone growth, and minimizes the risk of adverse reactions such as inflammation or infection. Advanced materials like PEEK and bioactive coatings such as HA have been explored to address these challenges, providing implants with both the mechanical strength required for spinal support and the biological compatibility needed for integration with bone tissue. The successful design of spinal implants requires a comprehensive approach replicating the ECM's functional, morphological, and structural roles. Achieving this balance is the key to promoting the effective osseointegration, vascularization, and long-term stability of the implant. Ongoing advancements in biomaterials and 3DP technologies further enable the development of implants that better replicate the natural ECM, improving patient outcomes after spinal fusion and other orthopedic surgeries.

The key characteristic in scaffold design is biocompatibility, which supports natural cell growth on the implant's surface. Biocompatible materials enable cells to adhere, proliferate, and differentiate, forming new tissue around the implant [127]. Equally important is the mechanical alignment of the implant with the surrounding bone, as the mechanical properties directly affect how the load is distributed [128]. If the implant is too stiff, it can lead to stress shielding, where the implant bears too much of the load, causing the nearby bone tissue to weaken and resorb. Conversely, if the implant is too flexible, it may not provide the structural support needed for healing. Thus, optimizing mechanical compatibility is essential not only for load transmission, but also for facilitating tissue regeneration [88,127,128].

Porosity is another critical factor for the long-term success of spinal implants. A suitable level of porosity allows for cell ingrowth, creating channels that support the transportation of nutrients and waste [106,129,130]. This feature is vital for promoting vascularization and the overall health of the newly formed tissue. Additionally, the porosity of the implant enhances its osseointegration capabilities [129]. Implants with an open cellular structure provide more surface area for cells to attach, which encourages bone growth [130]. At the same time, a porous design can reduce implant stiffness, helping to alleviate stress shielding and reduce the degree of bone resorption around the implant site [106].

To achieve these goals, open cellular structures are increasingly used in orthopedic implants due to their increased surface area and capacity to support bone ingrowth. These structures are designed to reduce the implant's stiffness, promote better load sharing between the implant and the bone, and enhance the biological integration of the implant into the body [129,130]. By carefully designing the topological characteristics of the scaffold,

such as porosity, pore size, strut thickness, shape, and overall mechanical properties, implant developers can create devices that not only support bone regeneration, but also reduce the risk of long-term complications, such as bone resorption and implant loosening [89,129].

The pore size plays a particularly important role, as it must be large enough to allow cells and blood vessels to infiltrate the scaffold, while still providing sufficient mechanical stability [87]. Strut thickness and pore shape are also important design considerations, as these factors influence both the implant's structural integrity and its ability to interact with surrounding bone tissue [104,106]. Together, these variables affect the mechanical performance of the implant and its capacity to support the regeneration of healthy bone tissue.

Scaffold designs for orthopedic applications must effectively perform under prolonged physiological loading, while accommodating variations in bone healing rates, which differ significantly with age [131,132]. In younger individuals, bone fractures may take up to six weeks to support weight-bearing and approximately one year for full integration, while elderly individuals often experience much slower repair rates [132]. This variation necessitates the careful consideration of scaffold properties tailored to different patient profiles. A critical challenge lies in managing the balance between mechanical properties and structural functionality. Scaffolds that demonstrate promising mechanical performance in vitro often fail in vivo due to poor vascularization and insufficient cell infiltration [132]. Achieving efficient vascularization and cellular integration requires an optimal porous architecture that supports both mechanical stability and biological activity. Advanced testing protocols are essential to evaluate scaffold designs under conditions that replicate real-world physiological loading. These protocols should simulate cyclic loading, nutrient perfusion, and in vivo biochemical conditions to predict scaffold behavior accurately [132–134]. By addressing these challenges and integrating innovative materials, lattice designs can better support vascularization, cell infiltration, and prolonged physiological loading, ultimately improving outcomes in tissue engineering applications [131,133].

The success of spinal implants relies on a carefully balanced combination of functional, morphological, and structural design elements. Using advanced materials and open cellular structures in orthopedic implants allows for an improved biomechanical performance, enhanced osseointegration, and better patient outcomes [135]. Continued research into scaffold design, including the optimization of porosity and mechanical properties, will further advance the development of next-generation implants that better replicate the natural ECM and improve the success rates of orthopedic surgeries.

5.5. Topological Design of Cellular Scaffolds in Spinal and Other Orthopedic Implants

The design of cellular structures in orthopedic implants can vary significantly to replicate the characteristics of the natural bone ECM [89]. One of the most significant features in this design is the permeability of a porous scaffold, which plays a crucial role in facilitating blood flow through the implant. Adequate blood flow is essential for delivering nutrients and removing waste, processes that are vital for tissue regeneration and the overall success of osseointegration. Pore shape is the key factor influencing permeability and the implant's performance. For example, altering the pore shape from spherical to cylindrical can enhance the permeability of the scaffold, promoting better blood circulation and improving nutrient flow [89]. However, this design modification comes with disadvantages. Increasing permeability by altering the pore shapes often leads to a reduction in the implant's stiffness [135]. Reduced stiffness may compromise the structural integrity of the implant, making it less able to support mechanical loads, which is a concern, particularly in weight-bearing applications like spinal fusion. In addition to pore shape, the porosity and pore size of the scaffold significantly impact the degree of bone ingrowth [129,135]. The size and distribution of pores determine how deeply bone tissue

can infiltrate the scaffold and how much new bone can form within the implant. According to the literature, the optimal pore size for bone ingrowth has been reported to range from 50 to 1500 µm, with corresponding porosity levels between 40% and 70% [129,130]. These ranges reflect the diversity of materials and structures used in different implants, as well as variations in the specific anatomical requirements of the implant site. While smaller pore sizes may promote faster cell attachment and initial bone growth, larger pores are generally more favorable for long-term vascularization and deeper tissue integration, as shown in Figure 5.

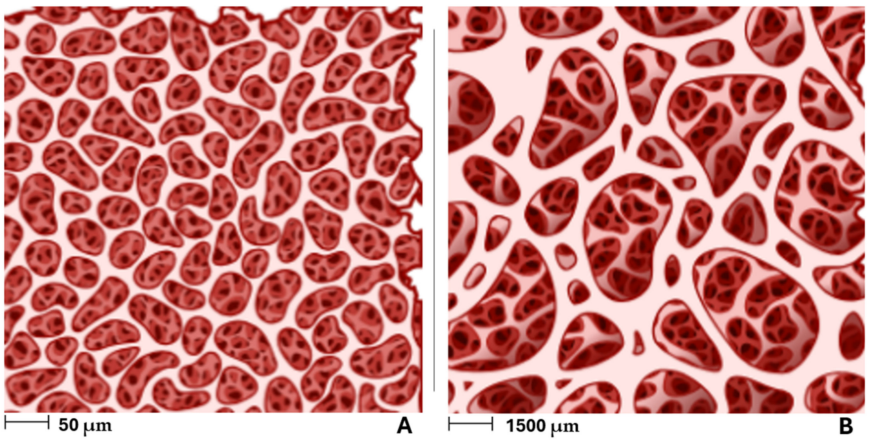

Figure 5. Shows comparison of smaller pore size (**A**) vs. larger pore size (**B**).

However, increasing the pore size can negatively affect the mechanical properties of the scaffold. For example, doubling the pore size has been shown to reduce the elastic modulus of the scaffold by over threefold [88,89]. This reduction in stiffness can weaken the scaffold's ability to bear physiological loads, highlighting the challenge of balancing mechanical strength with biological functionality. The ideal pore size and structure for achieving both biocompatibility and mechanical strength remains a topic of ongoing debate in the literature, as different materials and scaffold designs, whether stochastic or reticulated, exhibit varying responses to changes in pore size and shape [129]. Another aspect of the cellular structure design is the interplay between pore interconnectivity and scaffold architecture. A highly interconnected network of pores promotes not only bone ingrowth, but also vascularization, as the interconnected channels allow for the formation of new blood vessels [88]. This is critical for the long-term success of the implant, as adequate blood supply ensures continued bone remodeling and maintenance. However, balancing pore interconnectivity with sufficient mechanical stability remains a significant design challenge, as higher interconnectivity typically results in decreased stiffness. In conclusion, the topological design of cellular structures in orthopedic implants is a complex and finely tuned process. Designers and researchers must carefully consider factors, such as pore shape, size, porosity, and interconnectivity, to optimize both the biological and mechanical performances of the scaffold. While advances in 3DP and biomaterials have allowed for greater customization and control over these variables, further research is necessary to fully understand the ideal design parameters for different clinical applications. Achieving the right balance between permeability, stiffness, and bone growth will continue to be the key focus in the development of next-generation orthopedic implants. Synthetic HA with a stoichiometric Ca/P molar ratio of 1.67 has been formulated to imitate the main inorganic component of the bone ECM—bone apatite. Nonetheless, bone apatite is non-stoichiometric with a Ca/P molar ratio of less than 1.67 and called calcium-deficient carbonated hydroxyapatite. Moreover, bone apatite includes various trace elements, such as Mg, Zn, and Sr, that replace some of the lattice's components, resulting in bone apatite

with beneficial impurities present in small quantities. The process of ion substitution occurs when an ion that has been introduced into a crystal lattice structure replaces an atom or ion that was already present in the lattice. This can happen when the introduced ion is of a similar size and charge as the ion replaces, allowing it to fit into the lattice without disrupting its overall structure. Doping involves attaching an extra ion to the crystal lattice's surface structure, which does not incorporate into the lattice itself, nor modify the unit cell parameters. This is unlike the case when a larger or smaller ion is directly substituted within the crystal lattice, which results in changes to the unit cell parameters. Determining whether substitution or doping has occurred is crucial, and analytical techniques such as X-ray diffraction (XRD) and X-ray photoelectron spectroscopy (XPS) can confirm the mechanism that has taken place.

5.6. Lattice Structures Using PAEK/PAEK Apatite Composites

PAEK composite lattice structures play a key role in advancing spinal and other orthopedic implants by combining mechanical strength, biocompatibility, and design flexibility, all of which are crucial for effective function and recovery [115]. The porous lattice design, often enhanced with bioactive fillers like HA, closely resembles natural trabecular bone, improving osseointegration and tissue integration. The integration of HA into PAEK matrices to enhance osseointegration is a challenging, yet promising area of research. Achieving the uniform distribution of HA within these polymer matrices is critical for optimizing their performance in biomedical applications, particularly in implants where bone integration is essential [41,136]. The traditional methods, such as injection molding, have been considered for this purpose, but they present limitations in ensuring homogeneity and stability of the composite material. Currently, there are insufficient data to pinpoint specific formulations or techniques that consistently deliver optimal results. The initial insights from the work of others suggest potential pathways for improvement, but these findings are preliminary and require further validation through systematic experimentation [28,137]. Additionally, understanding the influence of HA content, particle size, and distribution on the mechanical properties and biological performance of PAEK and PAEK/HA composites will be vital to achieving reliable and reproducible outcomes [128]. The ability to precisely control the pore size, shape, and interconnectivity within the lattice allows for structures that mimic the bone's microarchitecture, facilitating efficient bone growth and enhancing implant integration with the surrounding tissue [138]. This is particularly critical in spinal implants, as it improves implant stability and accelerates healing, significantly reducing the risk of implant failure. PAEK's mechanical properties, when reinforced with agents like HA or carbon fiber, can be finely tuned to replicate the stiffness and flexibility of natural bone [41,136]. The lattice structure optimizes these properties by better distributing mechanical loads, reducing the risk of stress shielding [139]. Optimizing the scaffold microstructure to balance bioactivity and mechanical strength without compromising either property is expected to involve a targeted series of experiments designed to evaluate these attributes. Given the lack of existing literature on this specific issue, employing Design of Experiment (DOE) methodologies or artificial intelligence (AI) could provide valuable guidance in identifying and refining an effective experimental approach [140–144]. These techniques may help determine optimal formulations or lattice structures to achieve the desired balance. The bone-like mechanical response of the lattice helps to prevent this, supporting natural bone remodeling and promoting long-term implant success [5,145]. Surface modifications, such as coating or texturing, can significantly enhance the bioactivity and mechanical interaction of implants with the surrounding tissue by improving cell adhesion, promoting osseointegration, and enhancing mechanical stability at the implant–tissue interface [146]. These techniques are particularly effective in line-of-sight applications,

where the uniform application of coatings or textures to the implant surface is feasible. However, in more complex structures such as lattice designs, the challenge of uniformly modifying internal surfaces arises [147]. In such cases, dip coating is one of the few viable methods, as it enables surface modifications to be applied uniformly across both the external and internal surfaces of the lattice [148]. This capability is critical for ensuring that the bioactivity and mechanical properties are consistently enhanced throughout the structure, particularly in areas where other methods may fail to reach or provide adequate coverage. Additionally, the customization possibilities afforded by 3D printing allow for implants to be tailored to the specific anatomical requirements of each patient. By creating lattice structures that match the patient's spine, implants are able to provide more effective support for spinal loads, reduce the likelihood of complications, and speed up recovery [149]. Another significant advantage of lattice structures is their ability to reduce the weight of spinal implants, without compromising strength or performance [5,6]. Spinal implants need to balance strength, flexibility, and minimal added weight [64]. Lattice structures allow for reduced material usage, while still maintaining the necessary structural integrity. This makes the implants lighter and more comfortable for patients, as well as reducing the production costs, particularly when manufactured through 3D printing. By optimizing both material efficiency and the performance, lattice-based PAEK composite implants offer a cost-effective solution that maintains the high standards required for medical devices [138]. PAEK composite lattice structures represent a promising advancement in spinal implant technology, enhancing biocompatibility, the mechanical performance, and customization, while reducing the weight and costs [118]. These innovations are paving the way for next-generation spinal surgeries, improving patient outcomes through more effective, personalized, and sustainable implant solutions.

6. Current Innovations in the Medical Device Industry Using PEEK and PEKK

Numerous companies manufacture spinal implants using PAEK polymers, capitalizing on their biocompatibility, mechanical strength, and imaging transparency. The key manufacturers are summarized in Table 7 below.

Table 7. Key manufacturers of spinal implants.

Company	Key Offerings	Special Features	Reference
Invibio Biomaterial Solutions	PEEK-OPTIMA polymers for spinal fusion	Supports bone integration; artifact-free imaging for CT, X-ray, and MRI	[150]
Zimmer Biomet	One2One™ system and other PEKK-based solutions for cranial and spinal implants	Exceptional mechanical strength; advanced 3D-printing technologies; patient-customized implants	[151]
Curiteva	Inspire™ 3D Porous PEEK HAFUSE™ Cervical Interbody System	3D-printed porous PEEK implants; improved spinal fusion outcomes and biocompatibility	[90]
Oxford Performance Materials (OPM)	OsteoFab® technology using PEKK for spinal implants	Biocompatibility; surface modifications for optimal performance	[152]
Prodorth	PROCORAL™ cervical disc prosthesis	Motion preservation for cervical disc surgeries.	[153]
Evonik Industries	VESTAKEEP® PEEK for spinal fusion implants, including K7C™ Cervical Spacer	Excellent mechanical properties; biocompatible; FDA-approved for spinal applications	[154]
Vy Spine	Products like OsteoVy PEKK Lumbar IBF made using OXPEKK™ material	Collaborates with OPM; 3D-printing technology for customized and innovative spinal solutions	[155]

These companies employ cutting-edge materials and advanced manufacturing technologies such as 3D printing to develop spinal implants optimized for individual patients' needs. Their innovative approaches play a pivotal role in advancing orthopedic and spinal care. By integrating PEEK and PEKK polymers, these manufacturers create implants that not only comply with rigorous regulatory requirements, but also enhance patient outcomes through an exceptional performance, biocompatibility, and customization. The unique combination of these polymers' properties has solidified their status as preferred materials for the development of next-generation medical devices.

Compared to titanium and Co-Cr alloys, which have long been the preferred materials for spinal implants, PAEK materials offer several key advantages. While titanium and Co-Cr alloys are valued for their strength and durability, they can present challenges with imaging, often causing artifacts in X-rays, CT scans, and MRIs [22]. In contrast, PEEK and PEKK polymers are transparent in these images, allowing for clearer and more accurate diagnostics and monitoring. Moreover, titanium and Co-Cr alloys are relatively stiff, which can lead to stress shielding and negatively impact bone tissue [21,34]. PAEK materials, however, have mechanical properties similar to those of bone, fostering better integration and reducing the risk of implant failure [29]. Their superior biocompatibility further improves patient outcomes by lowering the likelihood of adverse reactions or inflammation, making them the increasingly favored choice in spinal implant and other orthopaedia development. PAEK/HA composites promise a long-term performance, offer excellent biocompatibility, and promote bone integration due to the HA component. The low density and fatigue resistance of PAEK make it suitable for orthopedic applications, particularly in medium-load situations [61,139]. However, its mechanical properties such as stiffness are worse than those of titanium, which may limit its use in high-load-bearing areas. Despite this, PAEK/HA implants generally exhibit good osseointegration and stability over time, with minimal wear or degradation under stress [63,91]. This makes them a viable option for applications requiring reduced weight and enhanced osteointegration, though titanium remains the preferred material for high-load implants.

7. Conclusions

This review explored the potential of 3D-printed PEEK and PEKK as promising alternatives to titanium as orthopedic implants, with a particular focus on spinal fusion applications. This review evaluated multiple aspects, including porous scaffold designs, advanced AM techniques, and the incorporation of bioactive agents such as HA into PEEK and PEKK. The primary objective was to understand how these factors contribute to improving the biological and mechanical properties of spinal fusion implants, with the goal of enhancing the patients' outcomes. This review identified significant progress in the development of PEEK/HA and PEKK/HA composites. HA, known for its ability to support bone growth and promote osseointegration, has shown potential in enhancing the bioactivity of PEEK and PEKK implants. The integration of HA into these polymers improves their compatibility with bone tissue, addressing one of the key limitations of the traditional polymers. Additionally, advances in additive manufacturing, particularly 3DP, have enabled the creation of complex porous scaffold designs. These scaffolds are critical for facilitating tissue integration and bone regeneration, both of which are vital for achieving successful spinal fusion.

The porous scaffold designs discussed in the review are essential for enhancing the interaction between the implant and surrounding bone tissue. By allowing for improved tissue ingrowth and bone formation, these designs are helping to overcome challenges associated with osseointegration. However, despite these advancements, this review emphasized the need for a deeper understanding of how the scaffold microstructure affects

the balance between bioactivity and mechanical strength. While porous structures can promote tissue integration, they may also compromise the mechanical stability of the implant. Striking the right balance between bioactivity and a good mechanical performance remains a critical challenge in the design of PEEK/HA and PEKK/HA implants. To ensure the long-term success and durability of these implants, more research is needed to address the gaps in knowledge, particularly regarding the mechanical performance of PEEK/HA and PEKK/HA scaffolds under physiological loads. In-depth studies focusing on the interplay between the scaffold microstructure, bioactivity, and mechanical strength are crucial for refining implant design. These studies should involve a combination of biological research, including in vitro and in vivo experiments, as well as comprehensive mechanical testing. The results will provide valuable insights into the clinical performance of 3D-printed PEEK and PEKK scaffolds, helping to optimize their use in spinal fusion and other orthopedic applications.

Moving forward, continued innovation in scaffold design and material composition will be the key to ensuring that 3D-printed PEEK and PEKK implants meet the stringent biological and mechanical requirements needed for successful orthopedic procedures. As research in this field progresses, these materials hold the potential to further transform spinal fusion and other orthopedic surgeries, providing more effective and personalized treatment options for patients.

Author Contributions: Conceptualization, A.R.B., J.W., A.G., K.S.-A., K.R. and R.M.; methodology, A.R.B., R.M., A.G. and J.W.; validation, A.R.B., J.W., A.G., K.S.-A. and K.R.; formal analysis, A.R.B. and R.M.; investigation, A.R.B., J.W., A.G., K.S.-A., K.R. and R.M.; resources, A.R.B.; data curation, A.R.B. and R.M.; writing—original A.R.B. and R.M.; writing—review and editing, A.R.B., J.W., A.G., K.S.-A., K.R. and R.M.; visualization, A.R.B. and R.M.; supervision, A.R.B., A.G., J.W., K.S.-A. and K.R.; project administration, A.R.B. All authors have read and agreed to the published version of the manuscript.

Funding: A.R.B. acknowledges the Royal Academy of Engineering for supporting him with the award of an Industrial Fellowship (IF2122\130).

Institutional Review Board Statement: Not applicable.

Informed Consent Statement: Not applicable.

Data Availability Statement: Not applicable.

Conflicts of Interest: The authors declare no conflicts of interest.

References

1. Maloo, L.M.; Toshniwal, S.H.; Reche, A.; Paul, P.; Wanjari, M.B. A Sneak Peek Toward Polyaryletherketone (PAEK) Polymer: A Review. *Cureus* **2022**, *14*, e31042. [CrossRef] [PubMed]
2. Bikas, H.; Stavropoulos, P.; Chryssolouris, G. Additive manufacturing methods and modelling approaches: A critical review. *Int. J. Adv. Manuf. Technol.* **2016**, *83*, 389–405. [CrossRef]
3. Šupová, M. Substituted hydroxyapatites for biomedical applications: A review. *Ceram. Int.* **2015**, *41*, 9203–9231. [CrossRef]
4. Rodzén, K.; Sharma, P.K.; McIlhagger, A.; Mokhtari, M.; Dave, F.; Tormey, D.; Sherlock, R.; Meenan, B.J.; Boyd, A. The Direct 3D Printing of Functional PEEK/Hydroxyapatite Composites via a Fused Filament Fabrication Approach. *Polymers* **2021**, *13*, 545. [CrossRef]
5. Tao, W.; Leu, M.C. Design of lattice structure for additive manufacturing. *Int. Symp. Flex. Autom.* **2016**, *2016*, 325–332. [CrossRef]
6. Wu, J.; Wang, W.; Gao, X. Design and Optimization of Conforming Lattice Structures. *IEEE Trans. Vis. Comput. Graph.* **2019**, *27*, 43–56. [CrossRef] [PubMed]
7. Rubin, D.I. Epidemiology and risk factors for spine pain. *Neurol. Clin.* **2007**, *25*, 353–371. [CrossRef]
8. Vassilaki, M.; Hurwitz, E.L. Insights in Public Health: Perspectives on Pain in the Low Back and Neck: Global Burden, Epidemiology, and Management. *Hawai'i J. Med. Public Health* **2014**, *73*, 122. Available online: https://pmc.ncbi.nlm.nih.gov/articles/PMC3998232/ (accessed on 4 December 2024).

9. Alhowimel, A.S.; Alodaibi, F.; Alshehri, M.M.; Alqahtani, B.A.; Alotaibi, M.; Alenazi, A.M. Prevalence and Risk Factors Associated with Low Back Pain in the Saudi Adult Community: A Cross-Sectional Study. *Int. J. Environ. Res. Public Health* **2021**, *18*, 13288. [CrossRef]
10. Spinal Implants And Devices Market Size Report. 2030. Available online: https://www.grandviewresearch.com/industry-analysis/spinal-implants-spinal-devices-market (accessed on 5 February 2024).
11. Reisener, M.-J.; Pumberger, M.; Shue, J.; Girardi, F.P.; Hughes, A.P. Trends in lumbar spinal fusion-a literature review. *J. Spine Surg.* **2020**, *6*, 752–761. [CrossRef]
12. Provaggi, E.; Capelli, C.; Leong, J.J.H.; Kalaskar, D.M. A UK-based pilot study of current surgical practice and implant preferences in lumbar fusion surgery. *Medicine* **2018**, *97*, e11169. [CrossRef]
13. Bones: Types, Structure, and Function. Available online: https://www.medicalnewstoday.com/articles/320444#Bone-cells (accessed on 11 March 2023).
14. Willems, N.M.B.K.; Langenbach, G.E.J.; Everts, V.; Zentner, A. The microstructural and biomechanical development of the condylar bone: A review. *Eur. J. Orthod.* **2014**, *36*, 479–485. [CrossRef]
15. Yuan, B.; Zhou, S.; Chen, X. Rapid prototyping technology and its application in bone tissue engineering. *J. Zhejiang Univ. Sci. B* **2017**, *18*, 303. [CrossRef] [PubMed]
16. Spinal Anatomy | Vertebral Column. Available online: https://www.spineuniverse.com/anatomy/vertebral-column (accessed on 11 March 2023).
17. Spine Structure & Function: Parts & Segments, Spine Problems, Spine Health. Available online: https://my.clevelandclinic.org/health/articles/10040-spine-structure-and-function (accessed on 11 March 2023).
18. Spinal Surgery-Fusion | Medtronic. Available online: https://www.medtronic.com/us-en/patients/treatments-therapies/considering-back-surgery/spinal-fusion.html (accessed on 24 October 2022).
19. Al Barbarawi, M.M.; Allouh, M.Z.; Qudsieh, S.M.; Barbarawi, A. Cervical decompressive laminectomy and lateral mass screw-rod arthrodesis: Surgical experience and analytical review of 4120 consecutive screws. *Br. J. Neurosurg.* **2021**, *35*, 480–485. [CrossRef] [PubMed]
20. Patel, N.; Gohil, P. A Review on Biomaterials: Scope, Applications & Human Anatomy Significance. *Int. J. Emerg. Technol. Adv. Eng.* **2012**, *2*, 91–101.
21. Bances, I.F.; Aparicio, P.; Antonio, M.; Vega, A. Evaluation of Titanium Serum Levels in Patients After Spine Instrumentation: Comparison Between Posterolateral and 360º Spinal Fusion Surgery. *Cureus* **2019**, *11*, e5451. [CrossRef]
22. Sarfraz, S.; Mäntynen, P.-H.; Laurila, M.; Rossi, S.; Leikola, J.; Kaakinen, M.; Suojanen, J.; Reunanen, J. Comparison of Titanium and PEEK Medical Plastic Implant Materials for Their Bacterial Biofilm Formation Properties. *Polymers* **2022**, *14*, 3862. [CrossRef]
23. Geetha, M.; Singh, A.K.; Asokamani, R.; Gogia, A.K. Ti based biomaterials, the ultimate choice for orthopaedic implants—A review. *Prog. Mater. Sci.* **2009**, *54*, 397–425. [CrossRef]
24. Wu, M.; Keil, A.; Constantin, D.; Star-Lack, J.; Zhu, L.; Fahrig, R. Metal artifact correction for x-ray computed tomography using kV and selective MV imaging. *Med. Phys.* **2014**, *41*, 121910. [CrossRef] [PubMed]
25. Carter, L.N.; Addison, O.; Naji, N.; Seres, P.; Wilman, A.H.; Shepherd, D.E.T.; Grover, L.; Cox, S. Reducing MRI susceptibility artefacts in implants using additively manufactured porous Ti-6Al-4V structures. *Acta Biomater.* **2020**, *107*, 338–348. [CrossRef] [PubMed]
26. Suphangul, S.; Rokaya, D.; Kanchanasobhana, C.; Rungsiyakull, P.; Chaijareenont, P. PEEK Biomaterial in Long-Term Provisional Implant Restorations: A Review. *J. Funct. Biomater.* **2022**, *13*, 33. [CrossRef] [PubMed]
27. Rodzeń, K.; McIvor, M.J.; Sharma, P.K.; Acheson, J.G.; McIlhagger, A.; Mokhtari, M.; McFerran, A.; Ward, J.; Meenan, B.J.; Boyd, A.R. The Surface Characterisation of Fused Filament Fabricated (FFF) 3D Printed PEEK/Hydroxyapatite Composites. *Polymers* **2021**, *13*, 3117. [CrossRef] [PubMed]
28. Almasi, D.; Iqbal, N.; Sadeghi, M.; Sudin, I.; Abdul Kadir, M.R.; Kamarul, T. Preparation Methods for Improving PEEK's Bioactivity for Orthopedic and Dental Application: A Review. *Int. J. Biomater.* **2016**, *2016*, 8202653. [CrossRef]
29. Manzoor, F.; Golbang, A.; Jindal, S.; Dixon, D.; McIlhagger, A.; Harkin-Jones, E.; Crawford, D.; Mancuso, E. 3D printed PEEK/HA composites for bone tissue engineering applications: Effect of material formulation on mechanical performance and bioactive potential. *J. Mech. Behav. Biomed. Mater.* **2021**, *121*, 104601. [CrossRef]
30. PEEK, vs. PEKK: Which High Performance Material Should You Choose?—3Dnatives. Available online: https://www.3dnatives.com/en/peek-vs-pekk-240620214/#! (accessed on 28 November 2022).
31. Zol, S.M.; Alauddin, M.S.; Said, Z.; Ghazali, M.I.M.; Lee, H.E.; Farid, D.A.M.; Zahari, N.A.H.; Al-Khadim, A.H.A.; Abdul Aziz, A.H. Description of Poly(aryl-ether-ketone) Materials (PAEKs), Polyetheretherketone (PEEK) and Polyetherketoneketone (PEKK) for Application as a Dental Material: A Materials Science Review. *Polymers* **2023**, *15*, 2170. [CrossRef] [PubMed]
32. Vadapalli, S.M.S.; Sairyo, K.; Goel, V.K.; Robon, M.; Biyani, A.; Khandha, A.; Ebraheim, N.A. Biomechanical rationale for using polyetheretherketone (PEEK) spacers for lumbar interbody fusion-A finite element study. *Spine* **2006**, *31*, E992–E998. [CrossRef] [PubMed]

33. Niu, C.C.; Liao, J.C.; Chen, W.J.; Chen, L.H. Outcomes of interbody fusion cages used in 1 and 2-levels anterior cervical discectomy and fusion: Titanium cages versus polyetheretherketone (PEEK) cages. *Clin. Spine Surg.* **2010**, *23*, 310–316. [CrossRef] [PubMed]
34. All You Need to Know About PEEK for 3D Printing—3Dnatives. Available online: https://www.3dnatives.com/en/peek-3d-printing-060420204/#! (accessed on 4 December 2023).
35. Oladapo, B.I.; Zahedi, S.A.; Ismail, S.O.; Omigbodun, F.T. 3D printing of PEEK and its composite to increase biointerfaces as a biomedical material—A review. *Colloids Surf. B Biointerfaces* **2021**, *203*, 111726. [CrossRef]
36. Kim, I.Y.; Sugino, A.; Kikuta, K.; Ohtsuki, C.; Cho, S.B. Bioactive composites consisting of PEEK and calcium silicate powders. *J. Biomater. Appl.* **2009**, *24*, 105–118. [CrossRef] [PubMed]
37. Li, S.; Li, M.; Hu, J.; Li, G.; Wang, B.; Zhou, Z. A new strategy for PEEK-based biocomposites to achieve porous surface for bioactivity and adjustable mechanical properties for orthopedic stress matching. *Compos. Part A Appl. Sci. Manuf.* **2024**, *177*, 107909. [CrossRef]
38. Ratnayake, J.T.B.; Mucalo, M.; Dias, G.J. Substituted hydroxyapatites for bone regeneration: A review of current trends. *J. Biomed. Mater. Res. B Appl. Biomater.* **2017**, *105*, 1285–1299. [CrossRef] [PubMed]
39. Shepherd, J.H.; David; Shepherd, V.; Best, S.M. Substituted hydroxyapatites for bone repair. *J. Mater. Sci. Mater. Med.* **2012**, *23*, 2335–2347. [CrossRef]
40. Pokhrel, S.; Pokhrel, S. Hydroxyapatite: Preparation, Properties and Its Biomedical Applications. *Adv. Chem. Eng. Sci.* **2018**, *8*, 225–240. [CrossRef]
41. Zhou, H.; Lee, J. Nanoscale hydroxyapatite particles for bone tissue engineering. *Acta Biomater.* **2011**, *7*, 2769–2781. [CrossRef]
42. Fiume, E.; Magnaterra, G.; Rahdar, A.; Verné, E.; Baino, F. Hydroxyapatite for Biomedical Applications: A Short Overview. *Ceramics* **2021**, *4*, 542–563. [CrossRef]
43. Fernandez de Grado, G.; Keller, L.; Idoux-Gillet, Y.; Wagner, Q.; Musset, A.-M.; Benkirane-Jessel, N.; Bornert, F.; Offner, D. Bone substitutes: A review of their characteristics, clinical use, and perspectives for large bone defects management. *J. Tissue Eng.* **2018**, *9*, 2041731418776819. [CrossRef] [PubMed]
44. Li, F.; Feng, Q.L.; Cui, F.Z.; Li, H.D.; Schubert, H. A simple biomimetic method for calcium phosphate coating. *Surf. Coat. Technol.* **2002**, *154*, 88–93. [CrossRef]
45. Bhatt, R.A.; Rozental, T.D. Bone graft substitutes. *Hand Clin.* **2012**, *28*, 457–468. [CrossRef] [PubMed]
46. Roberts, T.T.; Rosenbaum, A.J. Bone grafts, bone substitutes and orthobiologics the bridge between basic science and clinical advancements in fracture healing. *Organogenesis* **2012**, *8*, 114–124. [CrossRef]
47. Wang, W.; Yeung, K.W.K. Bone Grafts and Biomaterials Substitutes for Bone Defect Repair A Review. *Bioact. Mater.* **2017**, *2*, 224–247. Available online: https://www.scirp.org/reference/referencespapers.aspx?referenceid=2366831 (accessed on 11 March 2023). [CrossRef] [PubMed]
48. Raimondi, S.; Zambon, A.; Ranieri, R.; Fraulini, F.; Amaretti, A.; Rossi, M.; Lusvardi, G. Investigation on the antimicrobial properties of cerium-doped bioactive glasses. *J. Biomed. Mater. Res. A* **2022**, *110*, 504. [CrossRef] [PubMed]
49. Russoni de Lima, I.; Gomes Alves, G.; Soriano, C.A.; Campaneli, A.P.; Gasparoto, T.H.; Schnaider Ramos, E., Jr.; de Sena, L.Á.; Malta Rossi, A.; Granjeiro, J.M. Understanding the impact of divalent cation substitution on hydroxyapatite: An in vitro multiparametric study on biocompatibility. *J. Biomed. Mater. Res. A* **2011**, *98*, 351–358. [CrossRef] [PubMed]
50. Sun, C.; Zhao, H.; Wang, L.; Zhang, J.; Zheng, J.; Yang, Z.; Huang, L.; Wang, L.; Liu, C.; Li, D.; et al. Additive manufactured polyether-ether-ketone composite scaffolds with hydroxyapatite filler and porous structure promoted the integration with soft tissue. *Biomater. Adv.* **2022**, *141*, 213119. [CrossRef] [PubMed]
51. Oladapo, B.I.; Ismail, S.O.; Oluwole, B.; Omigbodun, F.T.; Olawumi, M.A.; Muhammad, M.A. Lattice design and 3D-printing of PEEK with Ca10(OH)(PO4)3 and in-vitro bio-composite for bone implant. *Int. J. Biol. Macromol.* **2020**, *165*, 50–62. [CrossRef]
52. Von Wilmonsky, C.; Lutz, R.; Meisel, U.; Srour, S.; Rupprecht, S.; Toyoshima, T.; Nkenke, E.; Schlegel, K.A.; Pohle, D.; Münstedt, H.; et al. In Vivo Evaluation of ß-TCP Containing 3D Laser Sintered Poly(ether ether ketone) Composites in Pigs. *J. Bioact. Compat. Polym.* **2009**, *24*, 169–184. [CrossRef]
53. Ma, R.; Tang, S.; Tan, H.; Qian, J.; Lin, W.; Wang, Y.; Liu, C.; Wei, J.; Tang, T. Preparation, characterization, in vitro bioactivity, and cellular responses to a polyetheretherketone bioactive composite containing nanocalcium silicate for bone repair. *ACS Appl. Mater. Interfaces* **2014**, *6*, 12214–12225. [CrossRef]
54. Ma, R.; Tang, T. Current Strategies to Improve the Bioactivity of PEEK. *Int. J. Mol. Sci.* **2014**, *15*, 5426. [CrossRef] [PubMed]
55. Wu, X.; Liu, X.; Wei, J.; Ma, J.; Deng, F.; Wei, S. Nano-TiO2/PEEK bioactive composite as a bone substitute material: In vitro and in vivo studies. *Int. J. Nanomed.* **2012**, *7*, 1215–1225. [CrossRef]
56. Wong, K.L.; Wong, C.T.; Liu, W.C.; Pan, H.B.; Fong, M.K.; Lam, W.M.; Cheung, W.L.; Tang, W.M.; Chiu, K.Y.; Luk, K.D.K.; et al. Mechanical properties and in vitro response of strontium-containing hydroxyapatite/polyetheretherketone composites. *Biomaterials* **2009**, *30*, 3810–3817. [CrossRef]
57. Wang, L.; He, S.; Wu, X.; Liang, S.; Mu, Z.; Wei, J.; Deng, F.; Deng, Y.; Wei, S. Polyetheretherketone/nano-fluorohydroxyapatite composite with antimicrobial activity and osseointegration properties. *Biomaterials* **2014**, *35*, 6758–6775. [CrossRef]

58. Alqurashi, H.; Khurshid, Z.; Syed, A.U.Y.; Habib, S.R.; Rokaya, D.; Zafar, M.S. Polyetherketoneketone (PEKK): An emerging biomaterial for oral implants and dental prostheses. *J. Adv. Res.* **2020**, *28*, 87. [CrossRef] [PubMed]
59. Ding, N.; Zhou, M.; Cai, M. Synthesis and properties of novel copolymers of poly(ether ketone ketone) and poly(ether ether ketone ketone) containing amide and sulfone linkages. *High Perform. Polym.* **2013**, *25*, 126–134. [CrossRef]
60. Yuan, B.; Cheng, Q.; Zhao, R.; Zhu, X.; Yang, X.; Yang, X.; Zhang, K.; Song, Y.; Zhang, X.D. Comparison of osteointegration property between PEKK and PEEK: Effects of surface structure and chemistry. *Biomaterials* **2018**, *170*, 116–126. [CrossRef] [PubMed]
61. Song, C.-H.; Choi, J.-W.; Jeon, Y.-C.; Jeong, C.-M.; Lee, S.-H.; Kang, E.-S.; Yun, M.-J.; Huh, J.-B. Comparison of the Microtensile Bond Strength of a Polyetherketoneketone (PEKK) Tooth Post Cemented with Various Surface Treatments and Various Resin Cements. *Materials* **2018**, *11*, 916. [CrossRef]
62. Buck, E.; Li, H.; Cerruti, M. Surface Modification Strategies to Improve the Osseointegration of Poly(etheretherketone) and Its Composites. *Macromol. Biosci.* **2020**, *20*, 1900271. [CrossRef]
63. Poly-Ether-Ether-Ketone (Peek): A Review. Available online: https://www.researchgate.net/publication/365161148_POLY-ETHER-ETHER-KETONE_PEEK_A_REVIEW (accessed on 4 December 2024).
64. Handbook of Polymers—George Wypych—Google Books. Available online: https://books.google.co.uk/books?hl=en&lr=&id=mYZGEAAAQBAJ&oi=fnd&pg=PP1&dq=Wypych+G.+Elsevier;+Toronto:+2016.+Handbook+of+polymers.+&ots=HIYbk2J7hv&sig=ytR_Az5Dt5owRDJnIaWN7oJ0Mbs&redir_esc=y#v=onepage&q&f=false (accessed on 4 December 2024).
65. Cheng, K.; Shi, Z.; Wang, R.; Jiang, X.; Xiao, F.; Liu, Y. 3D printed PEKK bone analogs with internal porosity and surface modification for mandibular reconstruction: An in vivo rabbit model study. *Biomater. Adv.* **2023**, *151*, 213455. [CrossRef]
66. Oladapo, B.I.; Omigbodun, F.T.; Olawumi, M.A. 3D printing of PEEK–cHAp scaffold for medical bone implant. *Biodes. Manuf.* **2021**, *4*, 44–59. [CrossRef]
67. Yang, F.; Lin, F.; Song, C.; Zhou, C.; Jin, Z.; Xu, W. PBench: A Benchmark Suite for Characterizing 3D Printing Prefabrication. In Proceedings of the 2016 IEEE International Symposium on Workload Characterization (IISWC), Providence, RI, USA, 25–27 September 2016.
68. Rahimnejad, M.; Jahangiri, S.; Zirak Hassan Kiadeh, S.; Rezvaninejad, S.; Ahmadi, Z.; Ahmadi, S.; Safarkhani, M.; Rabiee, N. Stimuli-responsive biomaterials: Smart avenue toward 4D bioprinting. *Crit. Rev. Biotechnol.* **2024**, *44*, 860–891. [CrossRef] [PubMed]
69. Jahangiri, S.; Rahimnejad, M.; Nasrollahi Boroujeni, N.; Ahmadi, Z.; Motamed Fath, P.; Ahmadi, S.; Safarkhani, M.; Rabiee, N. Viral and non-viral gene therapy using 3D (bio)printing. *J. Gene Med.* **2022**, *24*, e3458. [CrossRef] [PubMed]
70. Wang, Y.; Zhou, Y.; Lin, L.; Corker, J.; Fan, M. Overview of 3D additive manufacturing (AM) and corresponding AM composites. *Compos. Part A Appl. Sci. Manuf.* **2020**, *139*, 106114. [CrossRef]
71. Liu, K.; Hu, N.; Yu, Z.; Zhang, X.; Ma, H.; Qu, H.; Ruan, C. 3D printing and bioprinting in urology. *Int. J. Bioprint.* **2023**, *9*, 325–342. [CrossRef]
72. Bellini, A.; Güçeri, S. Mechanical characterization of parts fabricated using fused deposition modeling. *Rapid Prototyp. J.* **2003**, *9*, 252–264. [CrossRef]
73. Baek, I.; Kwon, O.; Lim, C.M.; Park, K.Y.; Bae, C.J. 3D PEEK Objects Fabricated by Fused Filament Fabrication (FFF). *Materials* **2022**, *15*, 898. [CrossRef]
74. Saha, R.; Sarkar, M.; Choudhury, S.S.; Kumar, H.; Bhatt, G.; Bhattacharya, S. Evolution of 3d printing technology in fabrication of microfluidic devices and biological applications: A comprehensive review. *J. Micromanuf.* **2024**, *7*, 110–140. [CrossRef]
75. Jandyal, A.; Chaturvedi, I.; Wazir, I.; Raina, A.; Haq, M.I.U. 3D printing—A review of processes, materials and applications in industry 4.0. *Sustain. Oper. Comput.* **2022**, *3*, 33–42. [CrossRef]
76. Prabhakar, M.M.; Saravanan, A.K.; Lenin, A.H.; Leno, I.J.; Mayandi, K.; Ramalingam, P.S. A short review on 3D printing methods, process parameters and materials. *Mater. Today Proc.* **2021**, *45*, 6108–6114. [CrossRef]
77. Ahmad, M.N.; Yahya, A. Effects of 3D Printing Parameters on Mechanical Properties of ABS Samples. *Designs* **2023**, *7*, 136. [CrossRef]
78. 3D Printing Profile and 3D Printing Parameters: How to Choose Printing Settings to Print a Part | Roboze. Available online: https://www.roboze.com/en/resources/3d-printing-profile-and-3d-printing-parameters-how-to-choose-printing-settings-to-print-a-part.html (accessed on 26 January 2025).
79. Doshi, M.; Mahale, A.; Singh, S.K.; Deshmukh, S. Printing parameters and materials affecting mechanical properties of FDM-3D printed Parts: Perspective and prospects. *Mater. Today Proc.* **2022**, *50*, 2269–2275. [CrossRef]
80. Additive Manufacturing Process (3D Printing): 'A Critical Review of Techniques, Applications & Future Scope'. Available online: https://www.researchgate.net/publication/364997098_Additive_Manufacturing_Process_3D_Printing_A_Critical_Review_of_Techniques_Applications_Future_Scope (accessed on 26 January 2025).
81. Kristiawan, R.B.; Imaduddin, F.; Ariawan, D.; Ubaidillah; Arifin, Z. A review on the fused deposition modeling (FDM) 3D printing: Filament processing, materials, and printing parameters. *Open Eng.* **2021**, *11*, 639–649. [CrossRef]

82. Optimising 3D Printing Parameters for Success: Tips and Best Practices. Available online: https://www.objective3d.com.au/resource/blog/3d-printing-parameters-for-success-tips-and-best-practices/ (accessed on 26 January 2025).
83. Vidakis, N.; David, C.; Petousis, M.; Sagris, D.; Mountakis, N.; Moutsopoulou, A. The effect of six key process control parameters on the surface roughness, dimensional accuracy, and porosity in material extrusion 3D printing of polylactic acid: Prediction models and optimization supported by robust design analysis. *Adv. Ind. Manuf. Eng.* **2022**, *5*, 100104. [CrossRef]
84. Wittbrodt, B.; Pearce, J.M. The effects of PLA color on material properties of 3-D printed components. *Addit. Manuf.* **2015**, *8*, 110–116. [CrossRef]
85. Xue, W.; Krishna, B.V.; Bandyopadhyay, A.; Bose, S. Processing and biocompatibility evaluation of laser processed porous titanium. *Acta Biomater.* **2007**, *3*, 1007–1018. [CrossRef] [PubMed]
86. Pan, C.-T.; Lin, C.-H.; Huang, Y.-K.; Jang, J.S.C.; Lin, H.-K.; Kuo, C.-N.; Lin, D.-Y.; Huang, J.C. Design of Customize Interbody Fusion Cages of Ti64ELI with Gradient Porosity by Selective Laser Melting Process. *Micromachines* **2021**, *12*, 307. [CrossRef] [PubMed]
87. Abbasi, N.; Hamlet, S.; Love, R.M.; Nguyen, N.T. Porous scaffolds for bone regeneration. *J. Sci. Adv. Mater. Devices* **2020**, *5*, 1–9. [CrossRef]
88. Hollister, S.J. Porous scaffold design for tissue engineering. *Nat. Mater.* **2005**, *4*, 518–524. [CrossRef] [PubMed]
89. Home | Curiteva InspireTM Porous PEEK HA Fuse Technology. Available online: https://curiteva.com/ (accessed on 4 December 2024).
90. Barfeie, A.; Wilson, J.; Rees, J. Implant surface characteristics and their effect on osseointegration. *Br. Dent. J.* **2015**, *218*, E9. [CrossRef]
91. newdim3d.ca—Elevated Design & Creation. Available online: https://www.newdim3d.ca/ (accessed on 27 January 2025).
92. Singh, A.B. Transforming Healthcare: A Review of Additive Manufacturing Applications in the Healthcare Sector. *Eng. Proc.* **2024**, *72*, 2. [CrossRef]
93. Willemsen, K.; Nizak, R.; Noordmans, H.J.; Castelein, R.M.; Weinans, H.; Kruyt, M.C. Challenges in the design and regulatory approval of 3D-printed surgical implants: A two-case series. *Lancet Digit. Health* **2019**, *1*, e163–e171. [CrossRef]
94. *ISO 13485*; Medical Devices. International Organization for Standardization: Geneva, Switzerland, 2016. Available online: https://www.iso.org/iso-13485-medical-devices.html (accessed on 27 January 2025).
95. Chepelev, L.; Wake, N.; Ryan, J.; Althobaity, W.; Gupta, A.; Arribas, E.; Santiago, L.; Ballard, D.H.; Wang, K.C.; Weadock, W.; et al. Radiological Society of North America (RSNA) 3D printing Special Interest Group (SIG): Guidelines for medical 3D printing and appropriateness for clinical scenarios. *3D Print. Med.* **2018**, *4*, 1–38. [CrossRef]
96. Bhise, M.G.; Patel, L.; Patel, K. 3D Printed Medical Devices: Regulatory Standards and Technological Advancements in the USA, Canada and Singapore-A Cross-National Study. *Int. J. Pharm. Investig.* **2024**, *14*, 888–902. [CrossRef]
97. Morrison, R.J.; Kashlan, K.N.; Flanagan, C.L.; Wright, J.K.; Green, G.E.; Hollister, S.J.; Weatherwax, K.J. Regulatory Considerations in the Design and Manufacturing of Implantable 3D-Printed Medical Devices. *Clin. Transl. Sci.* **2015**, *8*, 594. [CrossRef] [PubMed]
98. Liverani, E.; Rogati, G.; Pagani, S.; Brogini, S.; Fortunato, A.; Caravaggi, P. Mechanical interaction between additive-manufactured metal lattice structures and bone in compression: Implications for stress shielding of orthopaedic implants. *J. Mech. Behav. Biomed. Mater.* **2021**, *121*, 104608. [CrossRef] [PubMed]
99. Arabnejad, S.; Johnston, B.; Tanzer, M.; Pasini, D. Fully porous 3D printed titanium femoral stem to reduce stress-shielding following total hip arthroplasty. *J. Orthop. Res.* **2017**, *35*, 1774–1783. [CrossRef] [PubMed]
100. Stanford, C.M.; Keller, J.C. The concept of osseointegration and bone matrix expression. *Crit. Rev. Oral Biol. Med.* **1991**, *2*, 83–101. [CrossRef] [PubMed]
101. Warnke, P.H.; Douglas, T.; Wollny, P.; Sherry, E.; Steiner, M.; Galonska, S.; Becker, S.T.; Springer, I.N.; Wiltfang, J.; Sivananthan, S. Rapid prototyping: Porous titanium alloy scaffolds produced by selective laser melting for bone tissue engineering. *Tissue Eng. Part C Methods* **2009**, *15*, 115–124. [CrossRef]
102. De La Plata, M.M.; Naval Gías, L.; Martos Díez, P.; Muñoz-Guerra, M.; González-García, R.; Cho Lee, G.-Y.; Castrejón-Castrejón, S.; Rodríguez-Campo, F.J. Osseointegrated implant rehabilitation of irradiated oral cancer patients. *J. Oral Maxillofac. Surg.* **2012**, *70*, 1052–1063. [CrossRef]
103. Otsuki, B.; Takemoto, M.; Fujibayashi, S.; Neo, M.; Kokubo, T.; Nakamura, T. Pore throat size and connectivity determine bone and tissue ingrowth into porous implants: Three-dimensional micro-CT based structural analyses of porous bioactive titanium implants. *Biomaterials* **2006**, *27*, 5892–5900. [CrossRef]
104. Li, Y.; Toraldo, G.; Li, A.; Yang, X.; Zhang, H.; Qian, W.-P.; Weitzmann, M.N. B cells and T cells are critical for the preservation of bone homeostasis and attainment of peak bone mass in vivo. *Blood* **2007**, *109*, 3839–3848. [CrossRef] [PubMed]
105. Zhang, B.; Guo, L.; Chen, H.; Ventikos, Y.; Narayan, R.J.; Huang, J. Finite element evaluations of the mechanical properties of polycaprolactone/hydroxyapatite scaffolds by direct ink writing: Effects of pore geometry. *J. Mech. Behav. Biomed. Mater* **2020**, *104*, 103665. [CrossRef]

106. Ashby, M.F.; Evans, A.G.; Fleck, N.A.; Gibson, L.J.; Hutchinson, J.W.; Wadley, H.N.G. Metal Foams: A Design Guide Library of Congress Cataloguing-in-Publication Data. Available online: http://www.iqytechnicalcollege.com/Metal_Foams.pdf (accessed on 17 December 2023).
107. Zok, F.W.; Latture, R.M.; Begley, M.R. Periodic truss structures. *J. Mech. Phys. Solids* **2016**, *96*, 184–203. [CrossRef]
108. Martínez, J.; Hornus, S.; Song, H.; Lefebvre, S. Polyhedral Voronoi diagrams for additive manufacturing. *ACM Trans. Graph.* **2018**, *37*, 15. [CrossRef]
109. Gibson, L.J.; Ashby, M.F. Cellular solids: Structure & properties, Oxford: Pergamon Press, ISBN: 0-08-036607-4, 1988, 357 + ix pages, $35.00. *Adv. Polym. Technol.* **1989**, *9*, 165–166. [CrossRef]
110. Chen, Z.; Shu, C.; Tan, D.S. A Truly Second-Order and Unconditionally Stable Thermal Lattice Boltzmann Method. *Appl. Sci.* **2017**, *7*, 277. [CrossRef]
111. Alkhader, M.; Vural, M. Mechanical response of cellular solids: Role of cellular topology and microstructural irregularity. *Int. J. Eng. Sci.* **2008**, *46*, 1035–1051. [CrossRef]
112. Korkmaz, M.E.; Gupta, M.K.; Robak, G.; Moj, K.; Krolczyk, G.M.; Kuntoğlu, M. Development of lattice structure with selective laser melting process: A state of the art on properties, future trends and challenges. *J. Manuf. Process.* **2022**, *81*, 1040–1063. [CrossRef]
113. Bajars, J.; Eilbeck, J.C.; Leimkuhler, B. 2D mobile breather scattering in a hexagonal crystal lattice. *Phys. Rev. E* **2020**, *103*, 022212. [CrossRef] [PubMed]
114. Ashby, M.F. The properties of foams and lattices. *Philos. Trans. R. Soc. A Math. Phys. Eng. Sci.* **2005**, *364*, 15–30. [CrossRef] [PubMed]
115. Murr, L.E.; Gaytan, S.M.; Medina, F.; Martinez, E.; Martinez, J.L.; Hernandez, D.H.; Machado, B.I. Characterization of Ti–6Al–4V open cellular foams fabricated by additive manufacturing using electron beam melting. *Mater. Sci. Eng. A* **2010**, *527*, 1861–1868. [CrossRef]
116. Deering, J.; Dowling, K.I.; DiCecco, L.A.; McLean, G.D.; Yu, B.; Grandfield, K. Selective Voronoi tessellation as a method to design anisotropic and biomimetic implants. *J. Mech. Behav. Biomed. Mater.* **2021**, *116*, 104361. [CrossRef]
117. Mahmoud, D.; Elbestawi, M.A. Lattice Structures and Functionally Graded Materials Applications in Additive Manufacturing of Orthopedic Implants: A Review. *J. Manuf. Mater. Process.* **2017**, *1*, 13. [CrossRef]
118. Fratzl, P.; Weinkamer, R. Nature's hierarchical materials. *Prog. Mater. Sci.* **2007**, *52*, 1263–1334. [CrossRef]
119. Zheng, X.; Lee, H.; Weisgraber, T.H.; Shusteff, M.; DeOtte, J.; Duoss, E.B.; Kuntz, J.D.; Biener, M.M.; Ge, Q.; Jackson, J.A.; et al. Ultralight, ultrastiff mechanical metamaterials. *Science* **2014**, *344*, 1373–1377. [CrossRef] [PubMed]
120. Cheng, X.Y.; Li, S.J.; Murr, L.E.; Zhang, Z.B.; Hao, Y.L.; Yang, R.; Medina, F.; Wicker, R.B. Compression deformation behavior of Ti–6Al–4V alloy with cellular structures fabricated by electron beam melting. *J. Mech. Behav. Biomed. Mater.* **2012**, *16*, 153–162. [CrossRef] [PubMed]
121. Gümrük, R.; Mines, R.A.W. Compressive behaviour of stainless steel micro-lattice structures. *Int. J. Mech. Sci.* **2013**, *68*, 125–139. [CrossRef]
122. Li, L.; Shi, J.; Zhang, K.; Yang, L.; Yu, F.; Zhu, L.; Liang, H.; Wang, X.; Jiang, Q. Early osteointegration evaluation of porous Ti6Al4V scaffolds designed based on triply periodic minimal surface models. *J. Orthop. Transl.* **2019**, *19*, 94–105. [CrossRef]
123. Ahmadi, S.M.; Yavari, S.A.; Wauthlé, R.; Pouran, B.; Schrooten, J.; Weinans, H.; Zadpoor, A.A. Additively Manufactured Open-Cell Porous Biomaterials Made from Six Different Space-Filling Unit Cells: The Mechanical and Morphological Properties. *Materials* **2015**, *8*, 1871. [CrossRef] [PubMed]
124. Van Bael, S.; Chai, Y.C.; Truscello, S.; Moesen, M.; Kerckhofs, G.; Van Oosterwyck, H.; Kruth, J.-P.; Schrooten, J. The effect of pore geometry on the in vitro biological behavior of human periosteum-derived cells seeded on selective laser-melted Ti6Al4V bone scaffolds. *Acta Biomater.* **2012**, *8*, 2824–2834. [CrossRef] [PubMed]
125. Hutmacher, D.W. Scaffolds in tissue engineering bone and cartilage. *Biomaterials* **2000**, *21*, 2529–2543. [CrossRef] [PubMed]
126. Zandi, M.; Mirzadeh, H.; Mayer, C.; Urch, H.; Baghaban Eslaminejad, M.; Bagheri, F.; Mivehchi, H. Biocompatibility evaluation of nano-rod hydroxyapatite/gelatin coated with nano-HAp as a novel scaffold using mesenchymal stem cells. *J. Biomed. Mater. Res. A* **2010**, *92*, 1244–1255. [CrossRef] [PubMed]
127. Gao, C.; Wang, C.; Jin, H.; Wang, Z.-H.; Li, Z.; Shi, C.; Leng, Y.; Yang, F.; Liu, H.; Wang, J. Additive manufacturing technique-designed metallic porous implants for clinical application in orthopedics. *RSC Adv.* **2018**, *8*, 25210–25227. [CrossRef]
128. Barbas, A.; Bonnet, A.S.; Lipinski, P.; Pesci, R.; Dubois, G. Development and mechanical characterization of porous titanium bone substitutes. *J. Mech. Behav. Biomed. Mater.* **2012**, *9*, 34–44. [CrossRef] [PubMed]
129. Campo, H.; Santamaria, X.; Cervelló, I.; Simón, C. Scaffolds for bioengineered uterus. In *Handbook of Tissue Engineering Scaffolds: Volume Two*; Elsevier: Amsterdam, The Netherlands, 2019; pp. 283–316. [CrossRef]
130. Suamte, L.; Tirkey, A.; Barman, J.; Babu, P.J. Various manufacturing methods and ideal properties of scaffolds for tissue engineering applications. *Smart Mater. Manuf.* **2023**, *1*, 100011. [CrossRef]

131. Chocholata, P.; Kulda, V.; Babuska, V. Fabrication of Scaffolds for Bone-Tissue Regeneration. *Materials* **2019**, *12*, 568. [CrossRef] [PubMed]
132. Loh, Q.L.; Choong, C. Three-Dimensional Scaffolds for Tissue Engineering Applications: Role of Porosity and Pore Size. *Tissue Eng. Part B Rev.* **2013**, *19*, 485. [CrossRef]
133. Arabnejad, S.; Johnston, R.B.; Pura, J.A.; Singh, B.; Tanzer, M.; Pasini, D. High-strength porous biomaterials for bone replacement: A strategy to assess the interplay between cell morphology, mechanical properties, bone ingrowth and manufacturing constraints. *Acta Biomater.* **2016**, *30*, 345–356. [CrossRef]
134. Ma, R.; Guo, D. Evaluating the bioactivity of a hydroxyapatite-incorporated polyetheretherketone biocomposite. *J. Orthop. Surg. Res.* **2019**, *14*, 32. [CrossRef] [PubMed]
135. Rodzeń, K.; Harkin-Jones, E.; Wegrzyn, M.; Sharma, P.K.; Zhigunov, A. Improvement of the layer-layer adhesion in FFF 3D printed PEEK/carbon fibre composites. *Compos. Part A Appl. Sci. Manuf.* **2021**, *149*, 106532. [CrossRef]
136. Santiago, C.C.; Yelamanchi, B.; Diosdado De la Peña, J.A.; Lamb, J.; Roguski, K.; Turzyński, F.; Faruqui, R.; Choo, K.; Du Plessis, A.; Sillani, F.; et al. Thermoplastic Extrusion Additive Manufacturing of High-Performance Carbon Fiber PEEK Lattices. *Crystals* **2021**, *11*, 1453. [CrossRef]
137. Hong, S.O.; Pyo, J.Y.; On, S.W.; Seo, J.Y.; Choi, J.Y. The Biocompatibility and the Effect of Titanium and PEKK on the Osseointegration of Customized Facial Implants. *Materials* **2024**, *17*, 4435. [CrossRef]
138. Enhancing Mechanical Properties of Materials Using Artificial Intelligence. Available online: https://www.researchgate.net/publication/372760348_Enhancing_Mechanical_Properties_of_Materials_Using_Artificial_Intelligence (accessed on 27 January 2025).
139. Jung, I.D.; Shin, D.S.; Kim, D.; Lee, J.; Lee, M.S.; Son, H.J.; Reddy, N.S.; Kim, M.; Moon, S.K.; Kim, K.T.; et al. Artificial intelligence for the prediction of tensile properties by using microstructural parameters in high strength steels. *Materialia* **2020**, *11*, 100699. [CrossRef]
140. Kibrete, F.; Trzepieciński, T.; Gebremedhen, H.S.; Woldemichael, D.E. Artificial Intelligence in Predicting Mechanical Properties of Composite Materials. *J. Compos. Sci.* **2023**, *7*, 364. [CrossRef]
141. Akbari, P.; Zamani, M.; Mostafaei, A. Machine learning prediction of mechanical properties in metal additive manufacturing. *Addit. Manuf.* **2024**, *91*, 104320. [CrossRef]
142. Grosselle, F.; Timelli, G.; Bonollo, F. Doe applied to microstructural and mechanical properties of Al–Si–Cu–Mg casting alloys for automotive applications. *Mater. Sci. Eng. A* **2010**, *527*, 3536–3545. [CrossRef]
143. Types of Lattices for Additive Manufacturing—The Terms All Engineers Need to Know—Gen3D. Available online: https://gen3d.com/news-and-articles/types-of-lattices-for-additive-manufacturing/ (accessed on 18 December 2023).
144. Kumaravelu, P.; Arulvel, S.; Kandasamy, J. Surface Coatings and Surface Modification Techniques for Additive Manufacturing. *Springer Tracts Addit. Manuf.* **2024**, 221–238. [CrossRef]
145. Jiang, P.; Rifat, M.; Basu, S. Impact of Surface Roughness and Porosity on Lattice Structures Fabricated by Additive Manufacturing-A Computational Study. *Procedia Manuf.* **2020**, *48*, 781–789. [CrossRef]
146. Deering, J.; Clifford, A.; D'Elia, A.; Zhitomirsky, I.; Grandfield, K. Composite dip coating improves biocompatibility of porous metallic scaffolds. *Mater. Lett.* **2020**, *274*, 128057. [CrossRef]
147. Chen, P.; Su, J.; Wang, H.; Yang, L.; Cai, H.; Li, M.; Li, Z.; Liu, J.; Wen, S.; Zhou, Y.; et al. Mechanical properties and microstructure characteristics of lattice-surfaced PEEK cage fabricated by high-temperature laser powder bed fusion. *J. Mater. Sci. Technol.* **2022**, *125*, 105–117. [CrossRef]
148. Understanding Spinal Anatomy: Intervertebral Discs. Available online: https://www.coloradospineinstitute.com/education/anatomy/intervertebral-discs/ (accessed on 11 March 2023).
149. Sacks, G.; Shah, V.; Yao, L.; Yan, C.; Shah, D.; Limeta, L.; DeStefano, V. Polyaryletherketones: Properties and applications in modern medicine. *Biomed. Technol.* **2024**, *6*, 75–89. [CrossRef]
150. PEEK Spinal Cage Solutions | Spinal Fusion Devices. Available online: https://invibio.com/en/application-areas/spine-and-orthopedics/spinal-cages (accessed on 4 December 2024).
151. Zimmer Biomet: Innovations in Orthopedic Care. Available online: https://www.zimmerbiomet.com/en (accessed on 4 December 2024).
152. Oxford Performance Materials' OsteoFab® 3D Printed PEKK Technology Focus of Study Published in The Spine Journal—Ortho Spine News. Available online: https://orthospinenews.com/2020/02/19/oxford-performance-materials-osteofab-3d-printed-pekk-technology-focus-of-study-published-in-the-spine-journal/ (accessed on 4 December 2024).
153. PRODORTH SPINE | Spine Products | Spinal Implants | TURKEY. Available online: https://www.prodorth.com/?gad_source=1&gclid=CjwKCAiAmMC6BhA6EiwAdN5iLT30a9Op0c__ax9cHTR-OkoYS1z0y_nQEeYHEEGbQCOnR9KpukOqHRoCPGQQAvD_BwE (accessed on 4 December 2024).

154. VESTAKEEP® Implant—PEEK Biomaterials from Evonik for Permanent Medical Implants—Evonik Industries. Available online: https://medical.evonik.com/en/materials-and-solutions/vestakeep-peek (accessed on 4 December 2024).
155. Vy Spine Announces FDA Clearance for its ClariVy OsteoVy PEKK Cervical IBF—SPINEMarketGroup. Available online: https://thespinemarketgroup.com/vy-spine-announces-fda-clearance-for-its-clarivy-osteovy-pekk-cervical-ibf/ (accessed on 4 December 2024).